

AD-A031 424

RCA LABS PRINCETON N J

F/G 20/12

RADIATION AND CHARGE INJECTION IN AL2O3 USING NEW TECHNIQUES.(U)

JAN 76 R J POWELL

F19628-74-C-0132

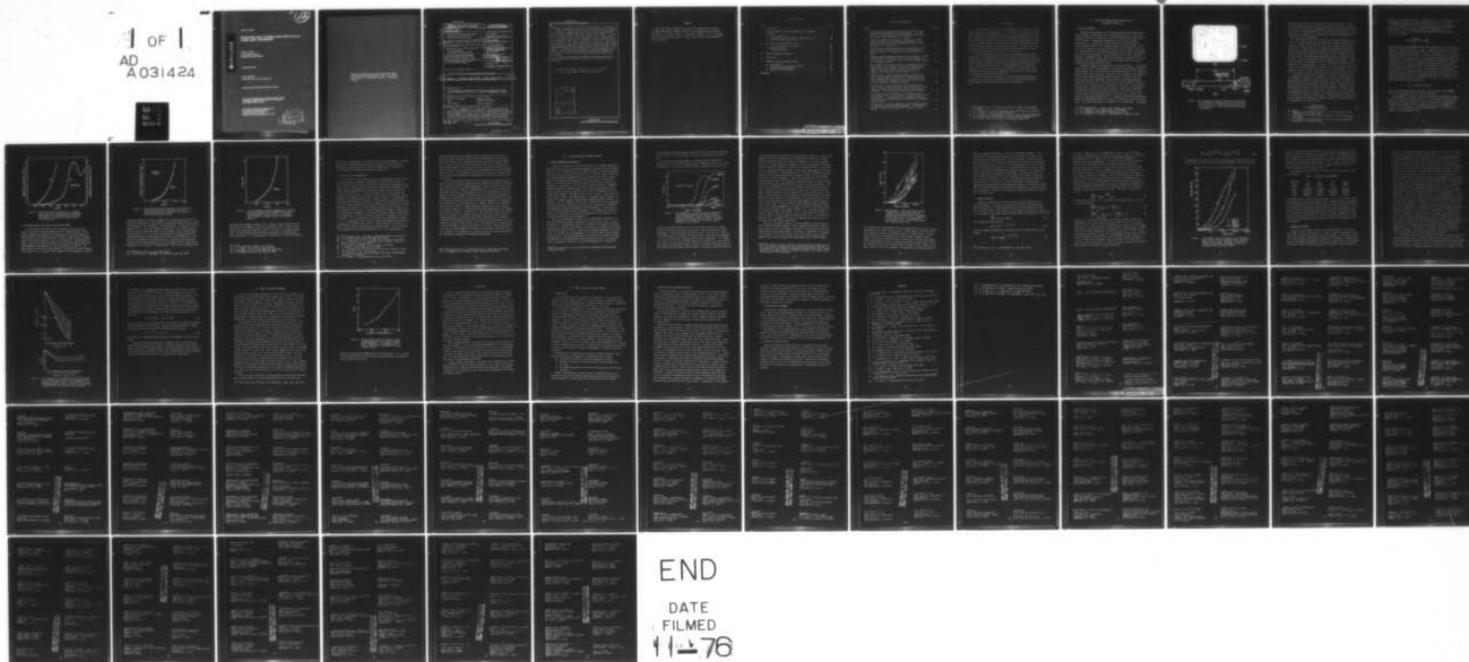
UNCLASSIFIED

PRRL-76-CR-8

AF6L-TR-76-0017

NL

1 OF 1  
AD  
A031424



76 (12)

AFGL-TR-76-0017

**RADIATION AND CHARGE INJECTION IN  $Al_2O_3$  USING NEW TECHNIQUES**

AD A031424

Richard J. Powell  
RCA LABORATORIES  
Princeton, New Jersey 08540

16 JANUARY 1976

**FINAL REPORT**  
18 December 1974 to 16 December 1975

Approved for public release; distribution unlimited.

This research was sponsored by the Defense Nuclear Agency under Subtask Z99QAXTDO33, Work Unit 42, entitled "HARDENED MIS DEVICES."

AIR FORCE GEOPHYSICS LABORATORY  
AIR FORCE SYSTEMS COMMAND  
UNITED STATES AIR FORCE  
HANSCOM AFB, MASSACHUSETTS 01731

D D C  
RECEIVED  
NOV 2 1976  
B

Qualified requestors may obtain additional copies from the Defense Documentation Center. All others should apply to the National Technical Information Service.

UNCLASSIFIED

SECURITY CLASSIFICATION OF THIS PAGE (When Data Entered)

19 REPORT DOCUMENTATION PAGE		READ INSTRUCTIONS BEFORE COMPLETING FORM
1. REPORT NUMBER 18 AFGL-TR-76-0017	2. GOVT ACCESSION NO.	3. RECIPIENT'S CATALOG NUMBER
4. TITLE (and Subtitle) 6 RADIATION AND CHARGE INJECTION IN Al <sub>2</sub> O <sub>3</sub> USING NEW TECHNIQUES.		5. TYPE OF REPORT & PERIOD COVERED Final Report (12-18-74 to 12-16-75)
7. AUTHOR(S) 10 Richard J. / Powell R. J. Powell		6. PERFORMING ORG. REPORT NUMBER 14 PRRL-76-CR-8
9. PERFORMING ORGANIZATION NAME AND ADDRESS RCA Laboratories Princeton, New Jersey 08540		8. CONTRACT OR GRANT NUMBER(s) 15 F19628-74-C-0132
11. CONTROLLING OFFICE NAME AND ADDRESS Air Force Geophysics Laboratory Hanscom AFB, Massachusetts 01731 Contract Monitor: Sven A. Roosild, LQD		10. PROGRAM ELEMENT, PROJECT, TASK AREA & WORK UNIT NUMBERS Subtask Z99QAXTD033 Work Unit 42
14. MONITORING AGENCY NAME & ADDRESS (if different from Controlling Office)		12. REPORT DATE 11 16 January 1976
		13. NUMBER OF PAGES 37 1260p.
		15. SECURITY CLASS. (of this report) Unclassified
		15a. DECLASSIFICATION/DOWNGRADING SCHEDULE N/A
16. DISTRIBUTION STATEMENT (of this Report) Approved for public release; distribution unlimited		
9 Final rept. 18 Dec 74 - 16 Dec 75		
17. DISTRIBUTION STATEMENT (for the abstract entered in Block 20, if different from Report)		
18. SUPPLEMENTARY NOTES This research was sponsored by the Defense Nuclear Agency under Subtask Z99QAXTD033, Work Unit 42, entitled "HARDENED MIS DEVICES."		
19. KEY WORDS (Continue on reverse side if necessary and identify by block number) Radiation hardening                      Charge injection SiO <sub>2</sub> High-field injection Hole trapping                                Optical properties		
20. ABSTRACT (Continue on reverse side if necessary and identify by block number) Optical transmission of unbacked thin films of thermally grown SiO <sub>2</sub> films was measured in the vacuum UV. The absorption data indicate a bandgap of 8.0 ± 0.2 eV for SiO <sub>2</sub> , and this value is confirmed by measurements of electron and hole photoconductivity and positive charging thresholds in MOS samples. Coincidence of the absorption and hole photoconductivity thresholds provides evidence that the		

DD FORM 1 JAN 73 1473

+ or -

UNCLASSIFIED

SECURITY CLASSIFICATION OF THIS PAGE (When Data Entered)

299 000 du

UNCLASSIFIED

SECURITY CLASSIFICATION OF THIS PAGE (When Data Entered)

20

uppermost valence levels in SiO<sub>2</sub> form a band, perhaps quite narrow, and most likely are dominated by oxygen 2p $\pi$  and silicon 3d atomic orbitals.

Vacuum ultraviolet radiation studies of steam-grown SiO<sub>2</sub> samples with different annealing temperatures show a rather sharp minimum in hole trapping at 1000°C. The results indicate the presence of at least two trap species whose densities vary oppositely with anneal temperature. A reasonable fit to the experimental results is obtained using a two-trap model, with trap cross sections of  $1.04 \times 10^{-13} \text{ cm}^2$  and  $6.5 \times 10^{-15} \text{ cm}^2$ . The former is believed to be associated with a species that diffuses into the oxide, particularly at high anneal temperatures, and the latter is associated with intrinsic interface trapping. Corona discharge experiments are inconsistent with the VUV results in that a monotonic increase in hole trap density with anneal temperature is observed. This is tentatively explained by the possible inability of this technique to fill traps with certain energy levels and spatial locations.

Included in this report is a summary of previous work on Al<sub>2</sub>O<sub>3</sub> which is described in earlier technical reports issued under this contract.

*\* 1.04 x 10 to the -13th power sq cm and  
6.5 x 10 to the -15th power sq cm*

ADDITION for	
NTIS	White Section <input checked="" type="checkbox"/>
DDC	Brief Section <input type="checkbox"/>
UNANNOUNCED	<input type="checkbox"/>
JUSTIFICATION	
BY	
DISTRIBUTION/AVAILABILITY CODES	
Dist.	AVAIL. NUMBER SPECIAL
A	

UNCLASSIFIED

SECURITY CLASSIFICATION OF THIS PAGE (When Data Entered)

## PREFACE

This Final Report describes work done at RCA Laboratories, Princeton, NJ, under Contract No. F19628-74-C-0132 in the Integrated Circuit Technology Center, J. H. Scott, Director. The Project Supervisor is K. H. Zaininger and the Project Scientist is R. J. Powell. The Air Force Project Monitor is Sven A. Roosild.

TABLE OF CONTENTS

Section	Page
I. INTRODUCTION . . . . .	7
II. OPTICAL PROPERTIES AND PHOTOCONDUCTIVITY IN THERMALLY GROWN SiO <sub>2</sub> . . . . .	8
A. Optical Absorption . . . . .	8
B. Photoconductivity and Charge Accumulation Spectra . . . . .	12
C. Discussion and Interpretation . . . . .	15
III. VACUUM ULTRAVIOLET RADIATION STUDIES . . . . .	17
A. Current Enhancement Experiments . . . . .	17
B. Trapping Kinetics . . . . .	21
C. Irreversible Effects . . . . .	24
IV. CORONA DISCHARGE EXPERIMENTS . . . . .	28
V. CONCLUSIONS . . . . .	30
VI. SUMMARY OF EARLIER CONTRACT REPORTS . . . . .	31
A. Introduction . . . . .	31
B. Vacuum Ultraviolet Radiation Studies . . . . .	32
C. Photoinjection Experiments . . . . .	33
D. High Field Charge Injection . . . . .	33
REFERENCES . . . . .	34

LIST OF ILLUSTRATIONS

Figure	Page
1. (a) Photograph of typical unbacked SiO <sub>2</sub> film, 580 Å thick, produced by etching through the silicon wafer. (b) Cross section of sample showing an actual measured oxide profile. The various crystalline planes are indicated . . . . .	9
2. Optical absorption coefficient of a thermally grown SiO <sub>2</sub> film as determined from transmission measurements. The expanded curve on the left corresponds to the scale on the left side of the illustration . . . . .	12
3. Photoconductivity spectra measured near threshold on an MOS structure with a 1034-Å SiO <sub>2</sub> film and a semitransparent Al-gate electrode. The yields for both bias polarities are given . . . . .	13
4. Charge accumulation spectrum measured near threshold on an MOS structure with a 1034-Å SiO <sub>2</sub> film and a semitransparent Al-gate electrode. The flatband shift produced by trapped charge is the measured quantity . . . . .	14
5. Time dependence of current during VUV irradiation for steam-grown samples with different helium anneal temperatures. Positive gate bias was used to produce an average field of 5 MV/cm. The photon energy was 10.2 eV and the SiO <sub>2</sub> <sup>-</sup> absorbed photon flux was 4 x 10 <sup>11</sup> cm <sup>-2</sup> s <sup>-1</sup> . . . . .	18
6. High-frequency (1 MHz) capacitance-voltage flatband shift versus time during VUV irradiation with positive gate bias and an average oxide field of 5 MV/cm. The samples are the same as used in the experiments illustrated in Fig. 5, and the same irradiation conditions were used . . . . .	20
7. Illustration of the fit of some of the experimental data of Fig. 6 with a theoretical model using two species of hole traps. The solid curves are theoretical and the points experimental. The trap parameters used are given in Table I . . . . .	23
8. (a) Illustration of the shape of the Si-SiO <sub>2</sub> barrier with a sheet charge of 10 <sup>13</sup> q cm <sup>-2</sup> located at various distances from the interface. (b) Variation of the tunneling distance $\chi_t$ with location of a charge sheet in the oxide for two different charge densities . . . . .	26
9. Flatband shift produced by negative corona discharge exposure as a function of helium anneal temperature. The samples are the same as those used in obtaining the results of Figs. 5 and 6 . . . . .	29

## I. INTRODUCTION

The spectral dependence of optical absorption of  $\text{SiO}_2$  through the fundamental absorption edge is important to interpretation of vacuum ultraviolet (VUV) transport and charging studies [1-3]. Accurate knowledge of the band-gap is important to analysis of electron bombardment experiments [4] and dielectric breakdown studies [5] in addition to its obvious importance to electronic structure studies. For these reasons, we have performed experiments on thin, unbacked films of thermally grown  $\text{SiO}_2$  films. The results of these experiments, along with photoconductivity and charge accumulation spectra, are presented and discussed in Section II of this report.

It has recently been shown [6] that processing parameters play an important role in determining the trap structure near the Si- $\text{SiO}_2$  interface. Studies of well-characterized MOS structures with steam-grown  $\text{SiO}_2$  films have been performed on samples with different post-oxidation anneal histories in order to determine the dependence on anneal temperature and ambient gas, hopefully to provide new insight into the nature of the hole trap. These results, which include current enhancement and flatband shift experiments, are presented and discussed in Section III.

Section IV contains the results of corona discharge experiments performed on the same series of samples used for the vacuum UV experiments. Similarities and differences are pointed out and discussed.

1. R. J. Powell and G. F. Derbenwick, IEEE Trans. Nuclear Science NS-19, 99 (1971).
2. A. G. Holmes-Siedle and I. Groombridge, Thin Solid Films 27, 165 (1975).
3. R. J. Powell, J. Appl. Phys. 46, 4557 (1975).
4. O. L. Curtis, J. R. Srour, and K. Y. Chiu, J. Appl. Phys. 45, 4506 (1974).
5. N. Klein, Advances in Electronics and Electron Physics 26, 309 (1971).
6. R. J. Powell, IEEE Trans. Nuclear Science NS-22, 2240 (1975).

## II. OPTICAL PROPERTIES AND PHOTOCONDUCTIVITY IN THERMALLY GROWN SiO<sub>2</sub>

### A. OPTICAL ABSORPTION

Transmission measurements on SiO<sub>2</sub> have previously been limited to thick (>1 mm) samples of fused silica [7] or crystalline quartz [8]. With such samples the absorption coefficient  $\alpha$  cannot be determined accurately above 50 cm<sup>-1</sup> because of experimental limitations such as scattered light. Philipp [9] has determined the optical properties of SiO<sub>2</sub> by means of a Kramers-Kronig analysis of his reflectance data. With this method, values of  $\alpha$  are not expected to be accurate much below 10<sup>5</sup> cm<sup>-1</sup> owing to the relative insensitivity of reflectance to absorption in this range. We have measured the optical transmission of thin unbacked films of SiO<sub>2</sub> to determine  $\alpha$  through the fundamental edge. These data indicated an energy gap of 8 eV for thermally grown SiO<sub>2</sub>. Measurements of the photoconductivity and positive charging thresholds confirm this value.

Transmission samples were prepared in the following manner: <100> silicon wafers, 0.15 mm thick, were polished on both sides and processed to produce a thick (5000-Å) film on the backside for masking purposes and a thin (900 Å to 2000 Å) oxide on the front side. Apertures, 1 mm in diameter, were etched in the back oxide using standard photoresist masking. The silicon was then etched through from the backside using a solution of Ethylenediamine and Pyrocatechol [10] at 110°C. The front side of a typical sample is shown in Fig. 1(a), and a cross section is illustrated in Fig. 1(b). The aperture in the back oxide is circular, but in the silicon it approaches a square with sloping sides because of the strong anisotropy in the silicon etch rates. The etch rates are approximately 50, 30, and 3 μm/h for the <100>, <110>, and <111> directions, respectively [10]. Therefore, etching proceeds rapidly beneath the masking oxide until <111> planes are formed and then practically stops. The crystalline planes are indicated in the illustration. The samples

7. D. F. Health and P. A. Sacher, *Appl. Optics* 5, 937 (1966).

8. A. A. Ballman, et al., *Appl. Optics* 7, 1387 (1968).

9. H. R. Philipp, *J. Phys. Chem. Solids* 32, 1935 (1971).

10. R. M. Finne and D. L. Klein, *J. Electrochem. Soc.* 114, 965 (1967).

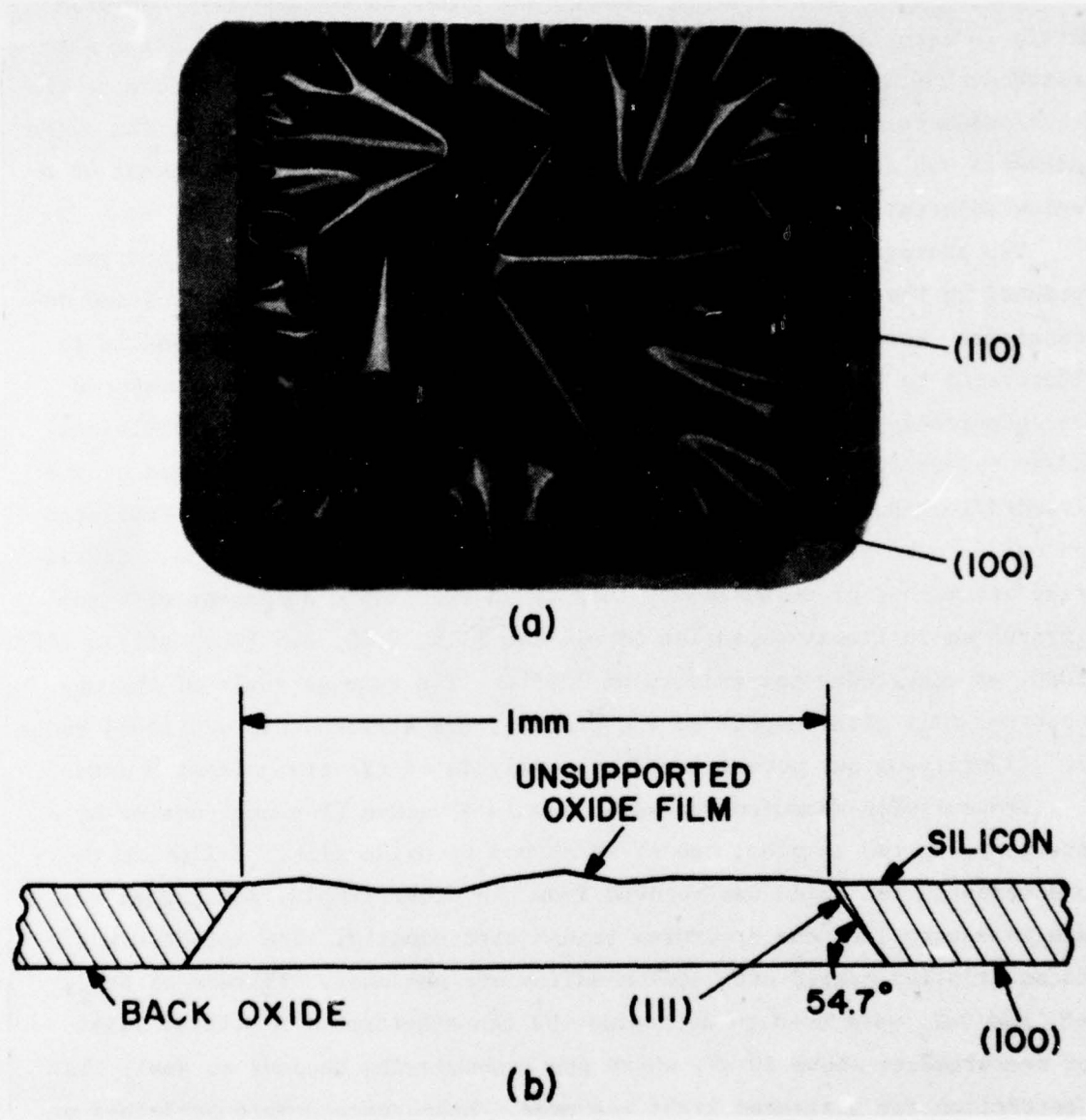


Figure 1. (a) Photograph of typical unbacked  $\text{SiO}_2$  film,  $580 \text{ \AA}$  thick, produced by etching through the silicon wafer. (b) Cross section of sample showing an actual measured oxide profile. The various crystalline planes are indicated.

are 5-mm square chips with the unsupported oxide in the center. Approximately 20 identical samples are formed simultaneously, the chip being separated during formation of the apertures. Since the exposed surface of the front oxide is etched somewhat (200 to 300 Å) during the process, the oxide thickness was determined after etching by an ellipsometer measurement of a region adjacent to the aperture.

The photograph of Fig. 1(a) is deceiving in that the strong contrast produced by the microscope gives the impression of large elevations and depressions. However, this is not the case, and a typical oxide profile is illustrated to scale in Fig. 1(b). Several oxide profiles were measured microscopically using a focusing stage with 1- $\mu$ m vertical scale divisions and an objective which produced a 1- $\mu$ m depth of focus. Calculation of the extended length of the oxide from such piecewise linear profiles indicated the oxide to be about 0.5% larger than the opening in the silicon. Considering our method of measurement, this is in reasonable agreement with the differences in linear expansion of silicon [11], 0.4%, and fused silica [12], 0.05%, at the growth temperature of 1000°C. The average angle of the unsupported film with respect to the plane of the silicon chip was found to be 4.5°, justifying our normal incidence analysis of the transmission data.

Transmission measurements were made in a vacuum UV monochromator by interchanging two samples, one of which had no oxide film. Following the measurements, the oxide was removed from the other sample, and checks were made to ensure that the apertures transmitted equally. The detector was a photomultiplier coated with sodium salicylate phosphor. Filters of BaF<sub>2</sub>, NaF, and CaF<sub>2</sub> were used to determine the contribution of scattered light for measurements above 10 eV, where the transmission becomes so small that a correction for scattered light was made. Measurements were performed on several samples with thicknesses of 580 Å and 2045 Å. The transmission of an unsupported film is given by [13]

$$T = \frac{(1-R)^2 (1+k^2/n^2)}{e^{-ad} - 2R \cos(\phi-\theta) - R^2 e^{-ad}} \quad (1)$$

11. *Handbook of Thermophysical Properties of Solid Materials*, Vol. 1, (MacMillan Co., New York, 1961).
12. T. A. Hahn and R. K. Kirby, *Thermal Expansion 1971 - AIP Conference Proceedings*.
13. O. S. Heavens, *Optical Properties of Thin Solid Films*, (Dover Publications, Inc., New York, 1965).

where  $R$  is the reflectance  $[(n-1)^2 + k^2]/[(n+1)^2 + k^2]$ ,  $n$  and  $k$  are the real and imaginary parts of the complex refractive index,  $n-ik$ ,  $\phi = 4\pi nd/\lambda$ ,  $\theta = 2\tan^{-1}[2k/(1-n^2-k^2)]$ ,  $d$  is the film thickness, and  $\alpha$  the absorption coefficient. In the usual range of transmission measurements  $k^2 \ll n^2$ ,  $e^{\alpha d} \gg R^2 e^{-\alpha d}$ , and  $\theta \simeq 0$ . Including these approximations, and solving Eq. (1) for  $\alpha$  we get

$$\alpha \simeq \frac{1}{d} \ln \left[ \frac{(1-R)^2}{T} + 2R\cos\phi \right] \quad (2)$$

The second term in the brackets results from interference in the film and is important where the transmission is large. Equation (2) was used to calculate  $\alpha$  from our transmission data from 8 eV to 10 eV, although above 9.5 eV the interference term has little effect. Values of  $R$  and  $n$  were obtained from the reflectance data of Philipp since it was previously established [1] that the reflectance of thermally grown  $\text{SiO}_2$  and fused silica are identical within experimental error. It should be noted that Philipp's values of  $n$  over this range should be quite accurate since  $k$  is small and  $R \simeq (n-1)^2/(n+1)^2$ . Since the absorption coefficient  $\alpha$  is  $4\pi k/\lambda$ , we can determine  $k$  for each photon energy to check the assumptions made in deriving Eq. (2) from Eq. (1). The approximations were found to be excellent except above 10.2 eV, where a correction was made for the factor  $(1+k^2/n^2)$  in Eq. (1). In this range  $\alpha$  was determined from a two-step iteration of

$$\alpha \simeq \frac{1}{d} \ln [(1-R)^2(1+k^2/n^2)/T] \quad (3)$$

and  $n$  was taken from the data of Philipp. This correction has a maximum effect of increasing  $\alpha$  about 5% at the 10.5-eV peak.

The absorption coefficient of  $\text{SiO}_2$  determined from transmission measurements on a 580-Å film is given in Fig. 2. It is seen that the absorption is still quite strong well below 9 eV, and just on the basis of magnitude the absorption above about 8.3 eV may be safely attributed to fundamental absorption. The data indicate an absorption threshold of 8 eV, which we interpret to be the bandgap of  $\text{SiO}_2$ .

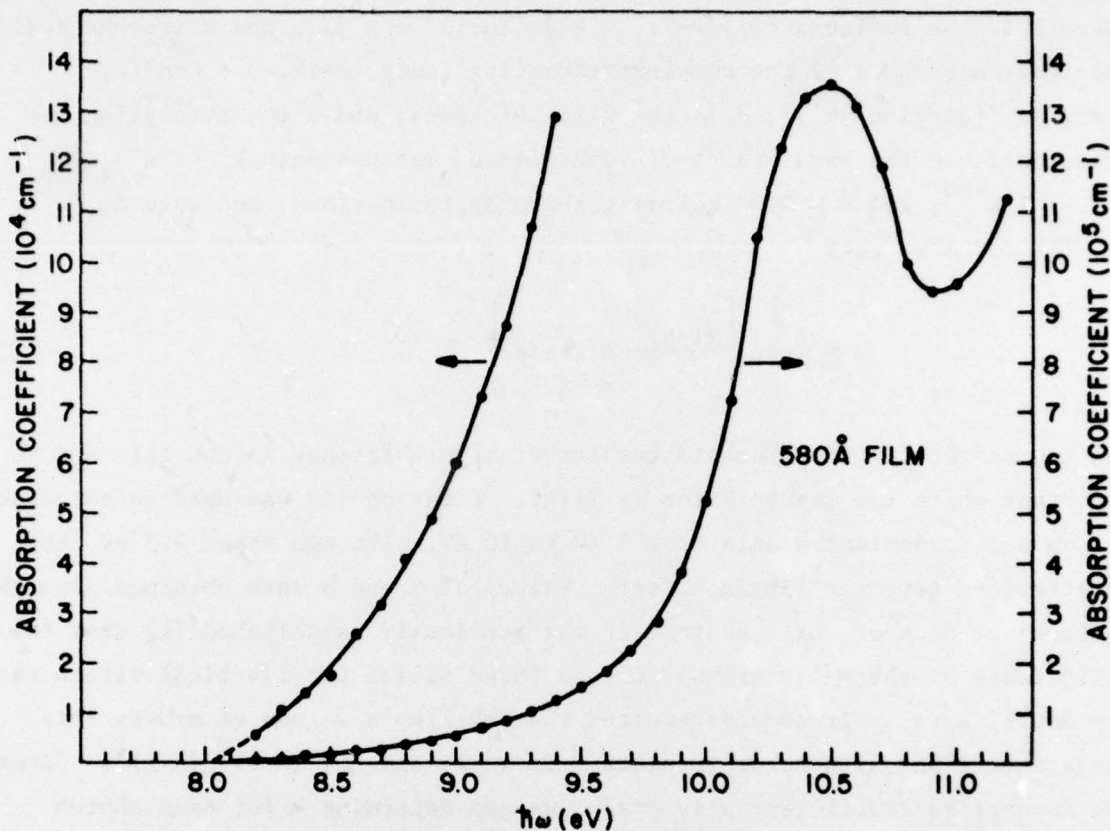


Figure 2. Optical absorption coefficient of a thermally grown  $\text{SiO}_2$  film as determined from transmission measurements. The expanded curve on the left corresponds to the scale on the left side of the illustration.

#### B. PHOTOCONDUCTIVITY AND CHARGE ACCUMULATION SPECTRA

It has recently been shown that hole trapping in  $\text{SiO}_2$  films varies widely with growth and anneal temperatures [6]. Using this fact, we have prepared samples with negligible hole trapping and large hole trapping for photoconductivity and charge accumulation spectra, respectively. The photoconductivity spectrum depicted in Fig. 3 was measured on a 1200-Å-thick MOS sample. With both positive and negative gate polarities, photocurrents were time-independent, and negligible charge accumulation was observed. The photoconductive yield shows a shape similar to the absorption, and the threshold is about 7.9 eV. In another 1200-Å sample, which was annealed to produce

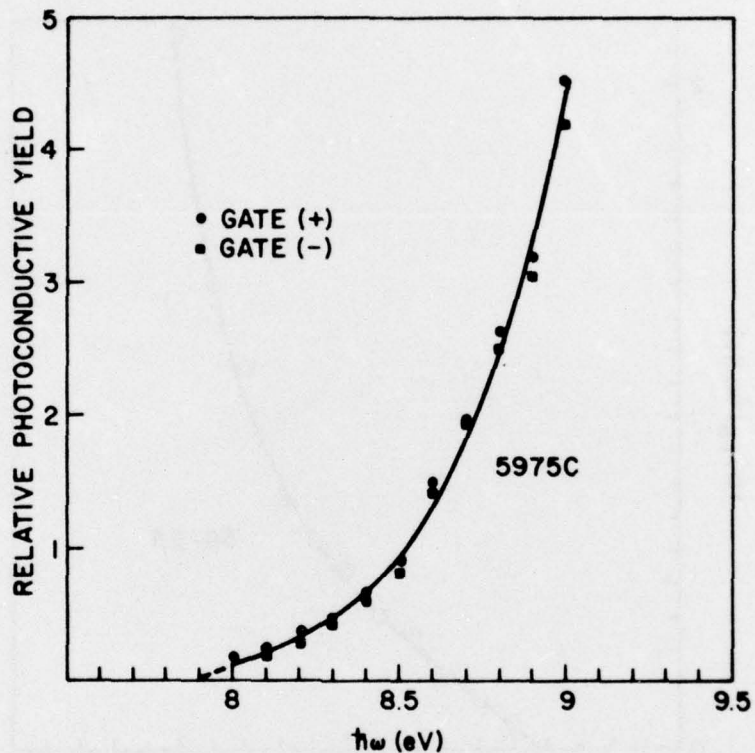


Figure 3. Photoconductivity spectra measured near threshold on an MOS structure with a 1034-Å  $\text{SiO}_2$  film and a semitransparent Al-gate electrode. The yields for both bias polarities are given.

large hole trapping, the spectral dependence of charge accumulation was determined by measuring the high-frequency capacitance-voltage shift  $\Delta V_{\text{FB}}$  versus photon energy for the same number of absorbed photons. This spectrum is illustrated in Fig. 4, and it also shows a threshold at 7.9 eV. Hence, we have shown in three separate experiments that the bandgap of  $\text{SiO}_2$  thermally grown on silicon is  $8.0 \pm 0.2$  eV. This value agrees with a previous estimate by Williams [14] based on transmission data of Groth and Weyssenhof [15]. However, such estimates were previously subject to question because the small absorption coefficients measurable with thick samples might be interpreted as absorption due to impurities or imperfections. Other previous estimates have

14. R. Williams, Phys. Rev. 140, A5669 (1965).

15. W. Groth and H. v. Weyssenhof, Z. Naturforsch. 11a, 165 (1956).

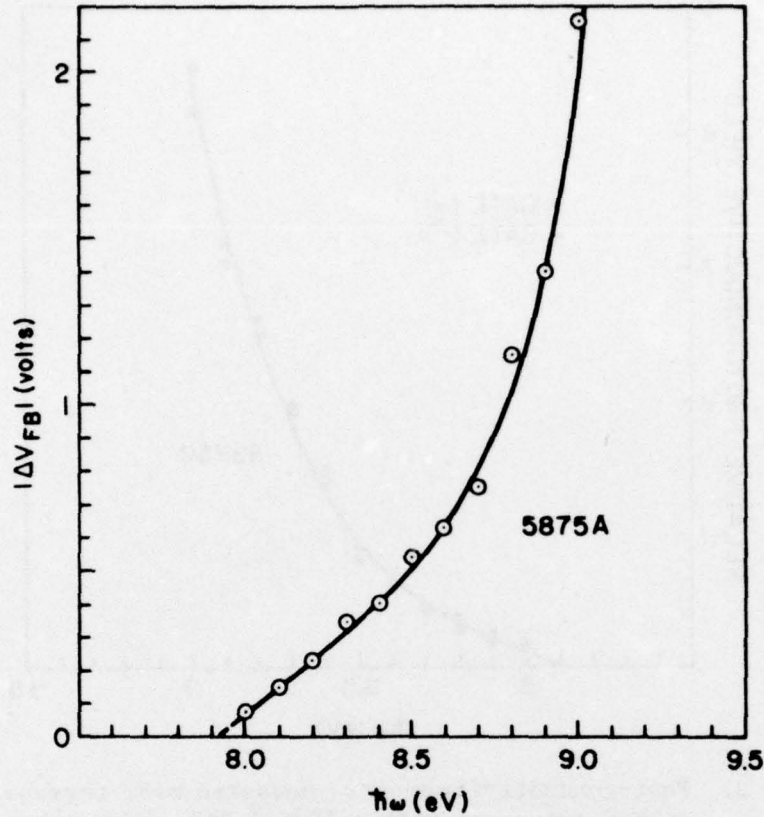


Figure 4. Charge accumulation spectrum measured near threshold on an MOS structure with a 1034-Å  $\text{SiO}_2$  film and a semitransparent Al-gate electrode. The flatband shift produced by trapped charge is the measured quantity.

placed the  $\text{SiO}_2$  bandgap as high as 11 eV. However, those estimates [16-19] were based on the assumption that the 10.5-eV peak in Fig. 2, which corresponds to the reflectance peak [9] at 10.3 eV, is due to an excitonic transition. The first band-to-band transition was assumed to lie energetically above the exciton. It is obvious from our results that if the 10.5-eV peak is

16. E. Loh, *Solid State Commun.* 2, 269 (1964).
17. A. R. Ruffa, *Phys. Stat. Sol.* 29, 605 (1968).
18. M. H. Reilly, *J. Phys. Chem. Solids* 31, 1041 (1970).
19. K. Platzöder, *Phys. Stat. Sol.* 29, K63 (1968).

excitonic, it is degenerate in energy with band-to-band transitions. Furthermore, since the photoconductivity near 10.5 eV shows no strong excitonic effects [20], it would seem that the only evidence for the interpretation is the temperature dependence reported by Platzöder [19].

### C. DISCUSSION AND INTERPRETATION

It is useful to consider the results of our experiments in light of the various theoretical predictions regarding the electronic energy levels in  $\text{SiO}_2$ . There have been a number of molecular orbital-type calculations of the energy levels in  $\text{SiO}_2$  and its polymorphs with tetrahedral coordination [21-24]. There is general agreement that the uppermost filled levels are associated with the 2p lone pair, or  $\pi$ , orbitals of oxygen (i.e., those orbitals not involved in the  $\sigma$ -bond with Si) and that the  $\sigma$ -electrons, being more strongly bonded, will have lower energy levels. However, there is a long-standing controversy regarding the importance of  $\pi$  bonding, which results from the overlap of the oxygen 2p $\pi$  orbitals and the originally empty 3d orbitals of silicon. Pauling [25] postulated the 3d-2p $\pi$  bonding to reduce the ionic nature of the Si-O bond below 50% to satisfy his electroneutrality principle. Recent positron annihilation experiments [26,27] support Pauling's argument, particularly for amorphous  $\text{SiO}_2$ , in which the effective charge of the oxygen atom is found to be about -0.6, in electronic units (50% ionicity corresponds to a charge of -1). The experimental and theoretical papers supporting 3d-2p $\pi$  bonding are too numerous to summarize here, and for a review the reader is referred to a paper by Revesz [28] and the references contained therein. On the other side of the argument are calculations by Gilbert, et al. [21], and Bennett and

20. T. H. DiStefano and D. E. Eastman, *Solid State Commun.* **9**, 2259 (1971).
21. T. L. Gilbert, et al., *Phys. Rev.* **B8**, 5977 (1973).
22. A. J. Bennett and L. M. Roth, *J. Phys. Chem. Solids* **32**, 1251 (1971).
23. G. A. D. Collins, D. W. J. Cruickshank, and A. Breeze, *J. Chem. Soc., Faraday Trans. II* **68**, 1189 (1972).
24. K. L. Yip and W. B. Fowler, *Phys. Rev.* **B10**, 1400 (1974).
25. L. Pauling, *J. Phys. Chem.* **56**, 361 (1952).
26. V. P. Prjanishnikov, et al., *Proc. IX International Congress on Glass*, Versailles, Vol. 1, pp. 119-131 (1971).
27. G. M. Bartenev, et al., *Izvestiya Akademii Nauk SSSR, Nerorganicheskie Materialy* **6**, 1553 (1970).
28. A. G. Revesz, *J. Non-Crystalline Solids* **11**, 309 (1973).

Roth [22] based on an  $\text{SiO}_2$  fragment and the  $\beta$ -cristobalite structure, respectively, which indicate relatively small 3d hybridization in the valence molecular orbitals. The calculations of Reilly [18] and the more extensive work of Yip and Fowler [24] unfortunately provide no direct evidence since these authors neglect d orbitals at the outset. However, the latter authors have noted that their poor agreement with experimental x-ray emission intensities may be due to their neglect of the silicon 3d orbitals. It seems likely that this may have contributed to the large ionicity they calculated for the  $\text{SiO}_4$  cluster.

The optical transitions involved in the absorption and photoconductivity spectra reported here must originate from the oxygen 2p lone pair ( $\pi$ ) orbitals, since it has been shown by ample experimental [21,29] and theoretical [18,21,24] evidence that the oxygen 2p  $\sigma$ -bonding band lies at least 5 eV below the uppermost filled level. The observation of hole photoconductivity over this range of  $h\nu$  with a threshold coincident with that of the optical absorption compels us to conclude that the upper valence levels are broadened into a band with sufficient orbital overlap that holes readily transport. The bonding in the uppermost band is most likely due to  $\pi$  bonding, which we have discussed above, since the  $2p\pi(\text{O}) - 3d(\text{Si})$  interaction is quite strong [23], whereas the overlap integral for  $\pi$  orbitals on neighboring oxygen atoms is much smaller even than that of their  $\sigma$  orbitals [21]. Also, holes are found to be trapped mostly near the  $\text{Si-SiO}_2$  interface [1,30], and the density of hole traps is strongly dependent on oxide growth and anneal temperatures [6]. These observations are inconsistent with models in which holes are presumed to be self-trapped in localized valence levels. As a final observation, the transmission of our 2045-Å sample is well below 0.05% for  $h\nu > 10$  eV. Hence, we must conclude that the photoluminescent efficiency in these films is less than 0.05%, and, therefore, the recombination in these films with the excitation levels of our experiments is dominated by nonradiative processes.

29. T. H. Distefano and D. E. Eastman, Phys. Rev. Letters 27, 1560 (1971).

30. R. Williams and M. H. Woods, J. Appl. Phys. 46, 695 (1975).

### III. VACUUM ULTRAVIOLET RADIATION STUDIES

#### A. CURRENT ENHANCEMENT EXPERIMENTS

It has been shown [3,6] that during irradiation of  $\text{SiO}_2$  MOS structures, holes travel in the  $\text{SiO}_2$ , and some are trapped in the vicinity of the negative electrode. This accumulation of space charge augments the average (applied) field, and when the interface field reaches 6 to 7 MV/cm, current enhancement is observed as electron tunneling from the electrode contributes to the current. This current enhancement phenomenon proves to be a very sensitive measure of the number and location of traps near the Si- $\text{SiO}_2$  and gate- $\text{SiO}_2$  interfaces. Furthermore, it also provides a sensitive method for comparing radiation sensitivity between samples with differing processing histories. In this section we present and discuss the results of experiments on well-characterized samples. The samples were grown on 1 ohm-cm n-type <100> silicon at 900°C in steam. Following oxidation, the samples were annealed for 15 minutes in ultrapure helium at temperatures ranging from 850° to 1100°C. In addition, one set of samples was also given a 15-min 500°C anneal in hydrogen. The wafers were then divided and metallized with 1-mm-diameter, 100-Å-thick (semitransparent) Al-gate electrodes for VUV experiments. No metallization was used for the corona discharge experiments. All samples were tested for mobile ion contamination using the bias-temperature stress technique, and contamination was found to be negligible.

The current enhancement phenomenon and its experimental implementation have been described in detail previously [1]; thus, it will only be outlined briefly here. The MOS sample under test is placed in a vacuum monochromator, biased with an appropriate gate bias, either positive or negative, and irradiated with VUV light of a photon energy that is strongly absorbed\* in the oxide film. One measures the time dependence of the total current flowing through the MOS device. The current measured at the initiation of radiation is just the electron or hole photocurrent flowing through the oxide. If the applied field is sufficient, eventually a current enhancement will be observed as

\*This is not essential, and the device may be irradiated with penetrating radiation as well.

holes accumulate near the negatively biased electrode, and electron tunneling current from this electrode becomes comparable to and exceeds the photocurrent.

The results of many experiments on steam-grown oxides, which were annealed in helium at various temperatures, are summarized in Fig. 5 for positive gate bias. The current flowing initially, as shown in this figure, is

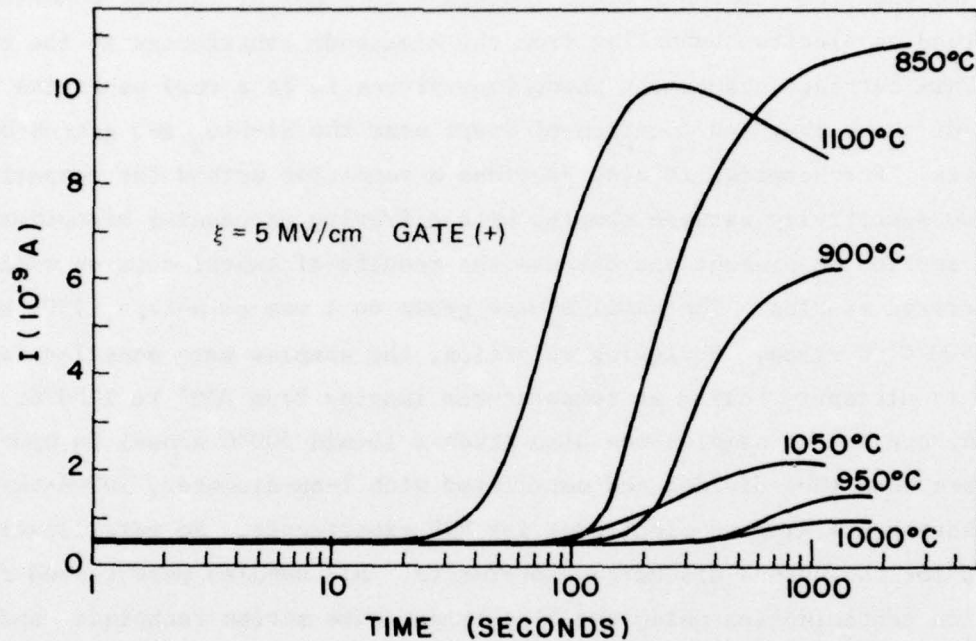


Figure 5. Time dependence of current during VUV irradiation for steam-grown samples with different helium anneal temperatures. Positive gate bias was used to produce an average field of 5 MV/cm. The photon energy was 10.2 eV and the  $\text{SiO}_2$ -absorbed photon flux was  $4 \times 10^{11} \text{ cm}^{-2}\text{s}^{-1}$ .

the hole photocurrent produced by the 10.2-eV photons, which are strongly absorbed in the  $\text{SiO}_2$  near the gate electrode. When sufficient space charge accumulates to raise the Si- $\text{SiO}_2$  interface field to the vicinity of 7 MV/cm, the current begins to increase. The curves of Fig. 5 show the time dependence of total oxide current for different helium anneal temperatures. It is important to point out that all of these samples have relatively few traps compared with those previously studied since no current enhancement is observed with applied fields less than about 4 MV/cm, whereas in previously reported results [6]

current enhancement was observed with applied fields as small as 1 MV/cm. Furthermore, one should recognize that the differences in the amount of space charge accumulation between the samples is magnified in the current enhancement by the strong current-field dependence of the tunnel-injection mechanism. The most striking observation to be made from the data of Fig. 5 is that there is a very strong and definite minimum in the current enhancement as a function of anneal temperature. Minimum enhancement is observed at 1000°C anneal temperature, and the temperature extremes at 850°C and 1100°C are about equally effective in current enhancement. These results indicate that the low- and high-temperature anneals have markedly increased the number of traps near the Si-SiO<sub>2</sub> interface which are effective\* in producing current enhancement. This statement is confirmed by the C-V curve flatband voltage shift data shown in Fig. 6. These data show that the flatband shifts at 10<sup>3</sup> s for the 850° and 1100°C samples are nearly twice as large as that of the 1000°C sample. Since there is ample evidence [1, 2] that charge is located mostly near the Si-SiO<sub>2</sub> interface following positive bias irradiation, this result implies that the amount of charge trapped in the 850° and 1100°C samples is about twice that of the 1000°C sample. The data of Fig. 6 show the same trends with temperature as the current enhancement data of Fig. 5. After 10<sup>3</sup>-s exposure, there is a definite minimum in the  $|\Delta V_{FB}|$  at 1000°C, and it increases markedly for lower and higher anneal temperatures. There is some crossing of curves at earlier times, and similar crossing is observed near 10<sup>2</sup>s in the current enhancement data. It appears that for short exposures the minimum  $|\Delta V_{FB}|$  is obtained with a 950°C anneal temperature.

There are two unusual effects to be noted regarding the differences between the 850° and 1100°C samples. First, focusing our attention on Fig. 5, we see that the 1100°C curve begins rising above the photocurrent about four times earlier than the 850°C sample. In addition, examination of the  $|\Delta V_{FB}|$  curves in Fig. 6 for  $t \gtrsim 100$  s reveals that for the same  $|\Delta V_{FB}|$  the 850°C sample has been irradiated about four times longer than the 1100°C sample.

\*The actual number of traps is difficult to ascertain because some may be so near to the silicon interface that they immediately empty by tunneling. It is suggested that the variation in temperature changes the density of traps which are either sufficiently far from the interface or have energy levels unfavorable for direct tunneling.

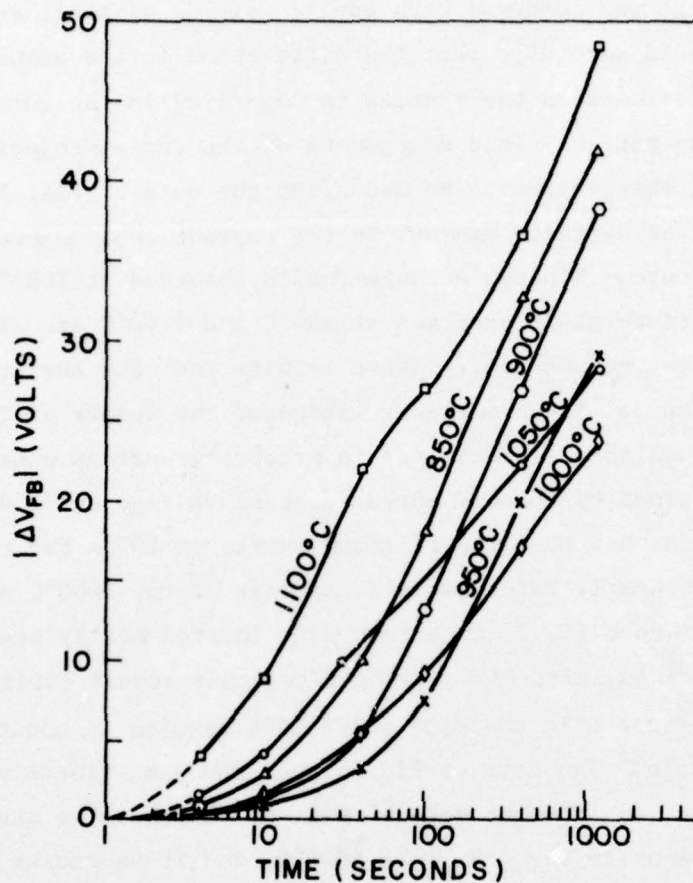


Figure 6. High-frequency (1 MHz) capacitance-voltage flatband shift versus time during VUV irradiation with positive gate bias and an average oxide field of 5 MV/cm. The samples are the same as used in the experiments illustrated in Fig. 5, and the same irradiation conditions were used.

If we consider that approximately equal hole photocurrents were used in the two experiments, this result indicates that the 1100°C sample is initially about four times more effective in trapping holes than the 850°C sample. An even larger difference is noted between the 1100° and 950°C samples in Fig. 6, where it is noted that the 950°C sample requires about ten times the exposure of the 1100°C sample in order to accumulate the same interface charge. It is also important to note that the final shifts obtained at 1000 s differ by only about a factor of two for all samples. We take this to be evidence that the

density of fillable traps does not vary much with anneal temperature. The large difference in trapping rate must then be attributed to differences in the capture cross section for holes. There is no reason to expect that the capture cross section of a specific trap should vary with anneal temperature; it is proposed that there are at least two different species of traps involved. Suppose, for example, that there is one trap species near the interface whose density decreases with temperature and a second trap with a much larger cross section whose density increases with temperature. The first trap might be associated with excess silicon near the interface [31], which, if associated with interface fixed charge, is known to decrease with increasing oxidation temperature [31]. The large cross section trap might be associated with a species which diffuses into the oxide much more rapidly at 1100°C than at 850°C. There is additional evidence that different trap species are involved, but before considering it further let us determine the approximate density and cross section of the traps.

#### B. TRAPPING KINETICS

Consider a distribution of traps located in a narrow region near the Si-SiO<sub>2</sub> interface. Let there be  $N_T$  traps per cm<sup>2</sup> of which  $N_T^+$  traps per cm<sup>2</sup> are filled with holes. Then the probability that a hole reaching the interface is trapped is  $(N_T - N_T^+) \cdot S$ , where  $S$  is the capture cross section. Letting  $J$  be the constant hole current density flowing through the interface, we can write

$$\frac{dN_T^+}{dt} = \frac{J}{q} \cdot (N_T - N_T^+) \cdot S \quad (4)$$

This equation has the solution:

$$N_T^+ = N_T \left( 1 - e^{-\frac{J}{q} \cdot S \cdot t} \right) \quad (5)$$

and if we express the densities of traps in terms of flatband shift, Eq. (5) becomes

$$\Delta V_{FB} = \Delta V_{FBF} \left( 1 - e^{-\frac{J}{q} \cdot S \cdot t} \right) \quad (6)$$

31. B. E. Deal, et al., J. Electrochem. Soc. 114, 266 (1967).

where  $\Delta V_{FB} = qN_T^+ d_{ox} / \epsilon_{ox}$  is the flatband shift at time  $t$ ,  $d_{ox}$  is the oxide thickness,  $\epsilon_{ox}$  is the dielectric constant, and  $\Delta V_{FBF} = qN_T^+ d_{ox} / \epsilon_{ox}$  is the flatband shift with all the traps filled. This simple model assumes that emission from traps is unimportant. It is well known that some hole traps near the silicon interface retain their charge for very short times so that they make no contribution to  $\Delta V_{FB}$ , which is measured typically minutes after each irradiation. Thus, the density  $N_T$  refers to the density of fillable interface traps, i.e., those which retain their charge for minutes or hours without appreciable detrapping. One can determine the trap density  $N_T$  and the capture cross section  $S$  by fitting Eq. (6) to experimental data. Unfortunately, it is not always possible to measure  $\Delta V_{FBF}$  directly because tunnel injection may prevent complete filling of traps, and the highest value of  $\Delta V_{FB}$  reached may be appreciably less than  $\Delta V_{FBF}$ . There is an alternate method for determining  $N_T$  and  $S$  from the data. Consider the derivative of Eq. (6):

$$\frac{d\Delta V_{FB}}{dt} = \Delta V_{FBF} e^{-\frac{JSt}{q}} \frac{J}{q} S \quad (7)$$

Evaluate the derivative at  $t = 0$  and some other convenient value of  $t$ , e.g.,  $t = q/JS$ ; then we get

$$\left. \frac{d\Delta V_{FB}}{dt} \right|_{t=0} = \Delta V_{FBF} \frac{J}{q} S = \frac{Jd_{ox}}{\epsilon_{ox}} N_T S \quad (8)$$

$$\left. \frac{d\Delta V_{FB}}{dt} \right|_{t=q/(JS)} = \Delta V_{FBF} \frac{J}{q} S e^{-1} = \frac{Jd_{ox}}{\epsilon_{ox}} N_T S e^{-1} \quad (9)$$

Clearly, we can determine the products  $N_T \cdot S$  from the initial slope of the experimental curve, and the time for which the slope is  $1/e$  of its initial value is just  $t = q/JS$ ; so we get  $S$  from this time. Hence,  $N_T$  and  $S$  are both determined. Using this technique, it was found that a good fit to the  $1100^\circ\text{C}$  curve in Fig. 6 was obtained for  $t \gtrsim 100$  with  $\Delta V_{FB} = 28(1 - e^{-t/28})$ . Since this equation saturates at  $\Delta V_{FB} = 28$ , the implication is that there are other traps with smaller  $S$  which account for the continued increase of  $\Delta V_{FB}$  for  $t > 100$ . Since there is reason to expect that there are at least two trap species involved, one should try to fit the data with an extension of Eq. (5), which applies for two noninteracting trap species:

$$N_T^+ = N_{T1} \left( 1 - e^{-\frac{J}{q} S_1 \cdot t} \right) + N_{T2} \left( 1 - e^{-\frac{J}{q} S_2 \cdot t} \right) \quad (10)$$

An approximate fit of Eq. (10) to some of the experimental data of Fig. 6 is shown in Fig. 7 for the 1100°, 950°, and 850°C samples. The fit was obtained

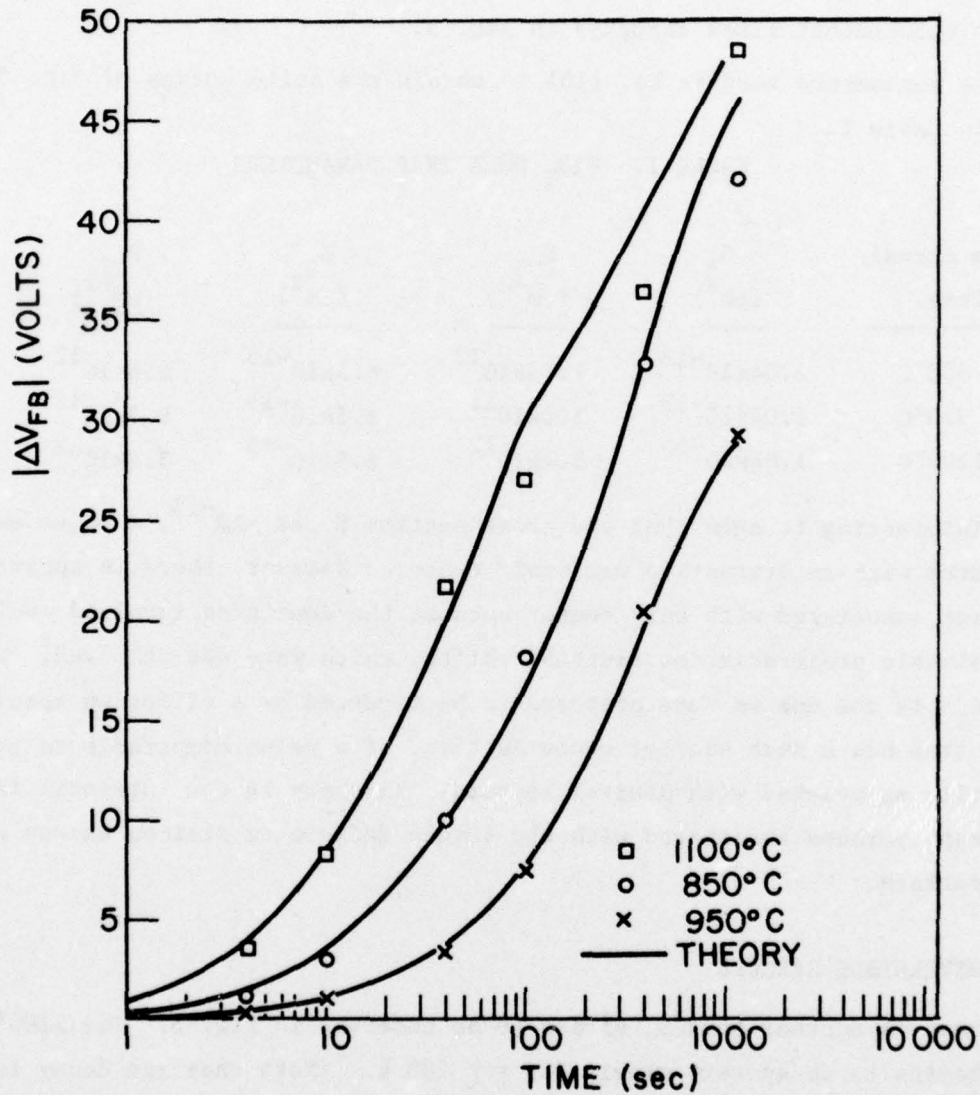


Figure 7. Illustration of the fit of some of the experimental data of Fig. 6 with a theoretical model using two species of hole traps. The solid curves are theoretical and the points experimental. The trap parameters used are given in Table I.

within the constraint that the same values of  $S_1$  and  $S_2$  are used for all three curves, and only the densities  $N_{T1}$  and  $N_{T2}$  were varied. The agreement is quite good, considering the simplicity of the model. Some of the discrepancy might be accounted for by the trap neutralization caused by the tunneling currents, especially for the 850° and 1100°C samples. In this regard, it should be noted that the kink in the 1100°C curve of Fig. 6 begins at about 40 s, where the current enhancement rises abruptly in Fig. 5.

The parameters used in Eq. (10) to obtain the solid curves of Fig. 7 are given in Table I.

TABLE I. SiO<sub>2</sub> HOLE TRAP PARAMETERS

He Anneal Temp.	$S_1$ (cm <sup>2</sup> )	$N_{T1}$ (cm <sup>-2</sup> )	$S_2$ (cm <sup>2</sup> )	$N_{T2}$ (cm <sup>-2</sup> )
850°C	$1.04 \times 10^{-13}$	$1.73 \times 10^{12}$	$6.5 \times 10^{-15}$	$8.6 \times 10^{12}$
950°C	$1.04 \times 10^{-13}$	$3.0 \times 10^{11}$	$6.5 \times 10^{-15}$	$6.3 \times 10^{12}$
1100°C	$1.04 \times 10^{-13}$	$5.4 \times 10^{12}$	$6.5 \times 10^{-15}$	$5.4 \times 10^{12}$

It is interesting to note that the cross section  $S_1$  is  $\sim 10^{-13}$ , a value usually associated with an attractive coulombic center. However, there is apparently no charge associated with this center because the densities involved would require sizable preirradiation flatband shifts, which were not observed. This trap ( $S_1$ ) is the one we have proposed to be produced by a diffusing species. The  $S_2$  trap has a much smaller cross section, of a value comparable to those ordinarily associated with neutral centers. This may be the intrinsic interface trap, perhaps associated with the oxygen deficit or silicon excess near the interface.

### C. IRREVERSIBLE EFFECTS

There is another unusual effect to be observed in Fig. 5. The 1100°C curve begins to decay very slowly for  $t \gtrsim 200$  s. (Note that the decay is much slower than the rise since the time scale is logarithmic.) This decay in the total current might be explained by a decrease in the number of trapped holes, causing a corresponding reduction in the field. However, this is not confirmed by the data of Fig. 6, which show a monotonic increase in  $|\Delta V_{FB}|$  during this

interval. It would appear that we have a dilemma: an increase in interface field and  $|\Delta V_{FB}|$  with a decrease in tunneling current. There are at least two possible explanations for this effect: (1) If some atomic species is ionized by the UV radiation, it could contribute a portion of the total current until depleted in the UV absorbing region. So an ionic component of current could decay with time. If the ions accumulate very near the Si-SiO<sub>2</sub> interface, they will not increase the tunneling current, although they will increase the flatband shift. The difficulty with this explanation is that it requires an ionic current of  $\sim 3 \times 10^{-9}$  A or  $\sim 3 \times 10^{-7}$  A/cm<sup>2</sup> to decay over several hundred seconds. This would result in the accumulation of more than  $10^{14}$  ions/cm<sup>2</sup> at the interface and unless some neutralization mechanism exists, this would produce a flatband shift of more than 500 volts. (2) When holes are trapped more than  $\sim 40$  Å from the Si-SiO<sub>2</sub> interface, they are effective in producing current enhancement and flatband shifts. On the other hand, charge trapped very near the interface has a much reduced effect on current enhancement. The effect of charge location on current enhancement is illustrated with the aid of Fig. 8(a), which shows the calculated shape of the conduction band edge near the Si-SiO<sub>2</sub> interface with an applied (average) field of 5 MV/cm and a sheet charge density of  $10^{13}$  q cm<sup>-2</sup> located at various distances from the interface. It is seen that the tunneling distance  $\chi_t$  from the silicon accumulation (or inversion) layer to the SiO<sub>2</sub> conduction band is markedly influenced by the location of the charge when it is within about 40 Å of the interface. In Fig. 8(b) we have plotted  $\chi_t$  versus charge location for two different charge densities. It is clear that charge located about 40 Å or more from the interface produces the largest current enhancement with only a small reduction in effectiveness with increasing distance up to 100 Å or more. However, since the tunneling current is exponentially dependent on  $\chi_t$ , its effectiveness is drastically reduced as charge moves nearer the interface. For example, increasing  $\chi_t$  from 40 Å to 50 Å will reduce the tunneling current by a factor of more than 1000.

The increasing  $|\Delta V_{FB}|$  in Fig. 6 proves that charge accumulation increases monotonically with time. In order to explain the decaying current in Fig. 4, we must hypothesize the motion of the charge centroid toward the Si-SiO<sub>2</sub> interface as accumulation continues. However, this motion of the centroid cannot be only the result of increased accumulation very near the interface; it must

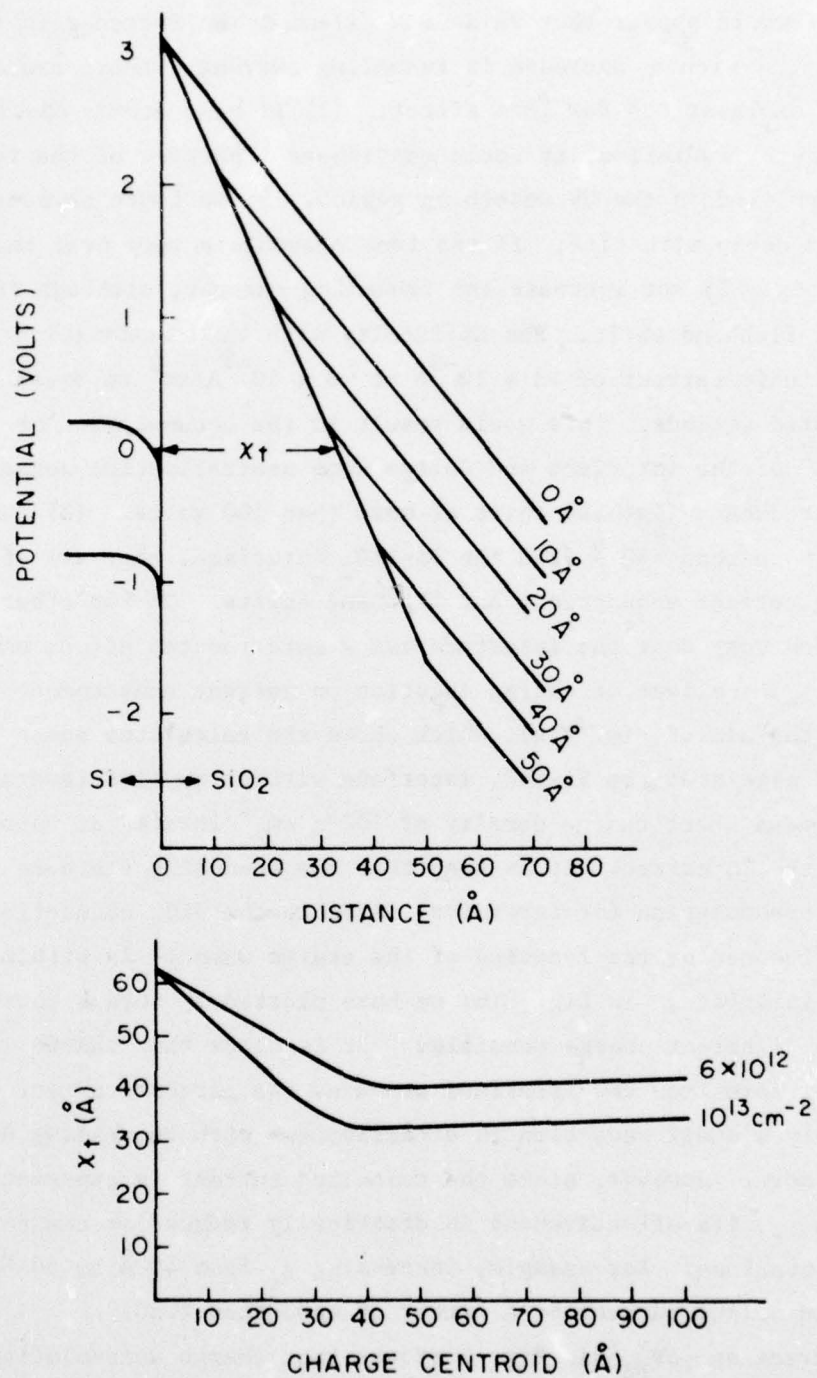
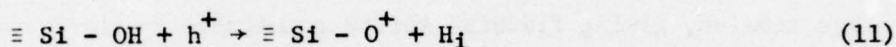


Figure 8. (a) Illustration of the shape of the Si-SiO<sub>2</sub> barrier with a sheet charge of  $10^{13} \text{ q cm}^{-2}$  located at various distances from the interface. (b) Variation of the tunneling distance  $x_t$  with location of a charge sheet in the oxide for two different charge densities.

be accompanied by a reduction in charge density at more effective densities further than  $\sim 40 \text{ \AA}$  from the interface. This would appear to require some change in the trap structure of the oxide with continuing irradiation. Since our knowledge of the microscopic nature of the hole trap near the Si-SiO<sub>2</sub> interface is still quite meager, it would be premature to assign a specific chemical reaction to the effect at this time. However, it is not difficult to imagine that the continuous flux of holes through this disordered interface region might produce chemical reactions which are essentially irreversible at room temperature. One possibility that comes to mind is expressed in the reaction:



In this reaction, a hole interacts with an Si-OH bond to liberate the hydrogen which may diffuse out of the oxide. The positive charge may then be annihilated by the injected electron flux leaving the center neutral.



The process is irreversible unless some source of hydrogen or protons is provided.

The current decay observed in Fig. 5 appears to be associated with the large cross section hole trap, since it is observed primarily in the 1100°C sample in which this trap predominates. This result provides further evidence that this trap is not intrinsic to the Si-SiO<sub>2</sub> interface but is associated with an impurity that has diffused in at the higher anneal temperatures.

#### IV. CORONA DISCHARGE EXPERIMENTS

In the corona discharge experiments, the surfaces of the unmetallized  $\text{SiO}_2$  films on silicon are charged with a negative corona in air. The corona tip is about 5 cm away from the oxide surface. Negative ions form near the tip and are rapidly thermalized. They are transported through the air and land on the outer surface of the oxide with negligible kinetic energy. The field across the oxide reaches about  $1.4 \times 10^7$  V/cm, which is sufficient to tunnel electrons from the hole trapping centers into the silicon directly or into the oxide conduction band [32]. When the corona is switched off the charge remains, giving flatband shifts comparable to those obtained with VUV irradiation. The flatband shifts are measured with a mercury probe.

The samples used in the experiments described here are portions of the same wafers used for the VUV experiments described in the previous section. The results are shown in Fig. 9, which displays the flatband shift versus helium anneal temperature. Since  $|\Delta V_{\text{FB}}|$  is proportional to the number of traps filled by this technique, there is an apparent inconsistency between these data and the VUV data of Fig. 6. The  $850^\circ\text{C}$  sample shows very little trapping in the corona experiment, but quite large trapping effects with the VUV exposure, particularly associated with the small cross section trap,  $S_2$ . If one examines the flatband shifts obtained with the VUV exposure at  $t = 10$  s in Fig. 6, he finds behavior qualitatively similar to that in Fig. 9, although the  $850^\circ\text{C}$  sample is out of place. These results suggest that the corona discharge experiment cannot fill certain traps available to holes, and these traps seem to be the ones with the small capture cross section. This disagreement between the two techniques might be explained if some traps are energetically near the  $\text{SiO}_2$  valence band edge (within  $\sim 3$  eV). Then it may be impossible for electrons to tunnel from these centers into the silicon because they may lie energetically opposite the Si- valence or forbidden bands even at  $1.4 \times 10^7$  V/cm. This is particularly true for traps located near the Si- $\text{SiO}_2$  interface.

While the results shown here are preliminary and have not been duplicated, they are significant in illustrating the importance of this technique in

---

32. M. H. Woods and R. Williams, to be published, J. Appl. Phys., Feb. 1976.

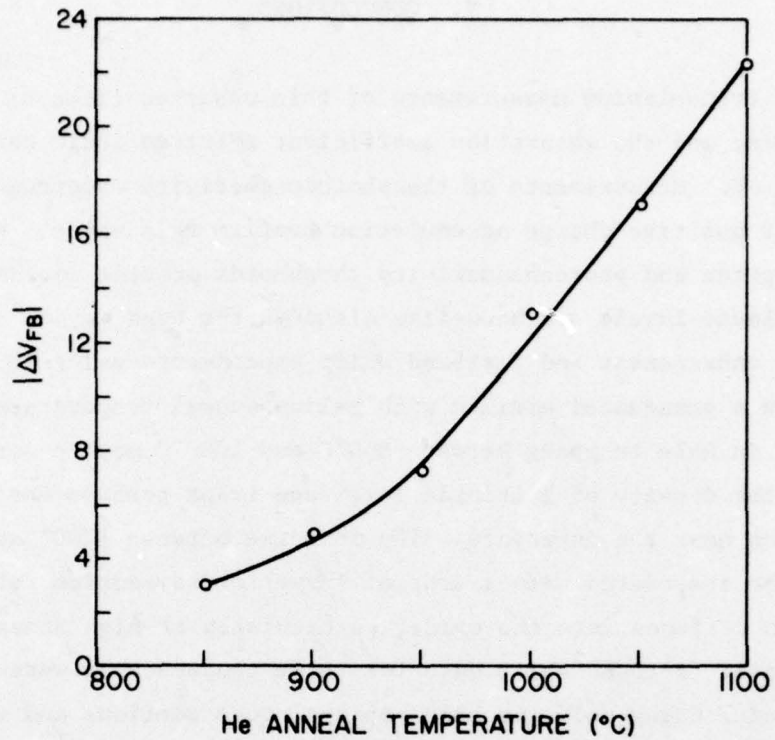


Figure 9. Flatband shift produced by negative corona discharge exposure as a function of helium anneal temperature. The samples are the same as those used in obtaining the results of Figs. 5 and 6.

sorting out the various characteristics of the hole traps. It is expected that the combination of the VUV and corona techniques will prove useful to future research in this area.

## V. CONCLUSIONS

Optical transmission measurements of thin unbacked films of  $\text{SiO}_2$  have been performed, and the absorption coefficient spectrum indicates a bandgap of  $8.0 \pm 0.2$  eV. Measurements of the photoconductivity spectrum and the threshold for positive charge accumulation confirm this value. Coincidence of the absorption and photoconductivity thresholds provides evidence that the uppermost valence levels are band-like although the band may be quite narrow.

Current enhancement and flatband shift experiments using 10.2-eV vacuum UV light show a pronounced minimum with helium anneal temperature near  $1000^\circ\text{C}$ . The decrease in hole trapping between  $850^\circ\text{C}$  and  $1000^\circ\text{C}$  may be associated with a change in the density of intrinsic interface traps perhaps associated with excess silicon near the interface. The increase between  $1000^\circ$  and  $1100^\circ\text{C}$  is believed to be associated with a trap of larger cross section related to a species which diffuses into the oxide, particularly at high anneal temperatures. The experimental flatband shift data for three temperatures were fitted with a two-trap model using only two hole capture cross sections and varying the density of the two traps. The cross sections are  $1.04 \times 10^{-13} \text{ cm}^2$  and  $6.5 \times 10^{-15} \text{ cm}^2$ , the first associated with a diffusing species, and the second with intrinsic interface trapping.

Some irreversible effects associated with the large cross section trap have been observed. A decay in the current enhancement with a corresponding increase in the flatband shift is believed to be the result of annihilation of some of the large cross section traps further from the interface during continued accumulation by the small cross section trap very near the interface. We have explained how such restructuring of the charge distribution can produce the experimental observation.

Corona discharge experiments on the same series of samples show a monotonic increase in  $\Delta V_{\text{FB}}$  with anneal temperature. This result is not entirely understood at this time and has been tentatively explained by the possible inability of this technique to fill certain traps, depending on their energy and spatial location.

## VI. SUMMARY OF EARLIER CONTRACT REPORTS

### A. INTRODUCTION

In this section we briefly summarize the research on  $\text{Al}_2\text{O}_3$  reported in earlier Scientific Reports; namely, in Technical Report No. AFCRL-TR-74-0330, dated 15 July 1974; Technical Report No. AFCRL-TR-75-0094, dated 16 January 1975; and Technical Report No. AFCRL-TR-75-0485, dated 17 July 1975.

The scientific work described in the aforementioned reports was undertaken with the purpose of applying new experimental techniques to develop models capable of explaining the phenomena of high-field charge injection and radiation-induced charging in pyrolytic  $\text{Al}_2\text{O}_3$  films suitable for MOS-gate insulators. The use of vacuum ultraviolet (VUV) radiation has proved to be extremely valuable to an understanding of radiation-induced charging in  $\text{SiO}_2$  films. Studies of  $\text{SiO}_2$ -MOS structures with bandgap light have revealed new information regarding the electronic processes in  $\text{SiO}_2$ . In particular, it has been shown that under positive gate bias holes transport to the vicinity of the Si- $\text{SiO}_2$  interface, where a significant number become trapped. The trapped charge enhances the interface field, resulting in electron tunneling currents that can be much larger than the photocurrents. These experiments have been extended to  $\text{Al}_2\text{O}_3$  in an effort to provide further understanding of the electronic processes involved in this material. In these reports, we describe the results and give an interpretation of vacuum UV experiments on pyrolytic  $\text{Al}_2\text{O}_3$  gate insulators.

Photoinjection of electrons has been used to provide information about three very important characteristics of the metal- $\text{Al}_2\text{O}_3$ -Si system,

- (1) The nature and location of electron trapping in the  $\text{Al}_2\text{O}_3$ .
- (2) The barrier energy for electron injection from the silicon into the  $\text{Al}_2\text{O}_3$ .
- (3) The scattering length for electrons in the  $\text{Al}_2\text{O}_3$  near the Si- $\text{Al}_2\text{O}_3$  interface.

Finally, the technique of constant-current charging has been used to evaluate the effects of processing temperature and  $\text{SiO}_2$  interlayers on the injection behavior of the Si- $\text{Al}_2\text{O}_3$  and Si- $\text{SiO}_2$ - $\text{Al}_2\text{O}_3$  interface regions.

## B. VACUUM ULTRAVIOLET RADIATION STUDIES

The energy threshold for electron-hole pair generation and radiation-induced positive charging was found to be approximately 7.8 eV. This value is significantly lower than previously predicted by others from interpretation of optical data. Our result indicates that their interpretation is probably incorrect. A decreasing flatband shift with photon energy was observed, and this is tentatively explained in terms of very small hole mobility, leaving holes trapped very near their birthsites.

The voltage dependence of flatband shift obtained under vacuum UV radiation shows a sharp maximum with voltage, and actually reverses sign for large gate voltages. This has been interpreted in terms of competition between electron-hole pair generation and electron injection from the electrodes at high interface fields.

Radiation-induced currents in aluminum oxide using strongly absorbed vacuum UV radiation have been measured. These currents show behavior similar to that which has been observed previously in  $\text{SiO}_2$  films; namely, there is a photocurrent component and a dark current component that is apparently produced by the tunneling of electrons into the film from the silicon electrode. Several differences are noted between these results and those reported for  $\text{SiO}_2$ . First, the photocurrent component is much smaller than in the case of  $\text{SiO}_2$ , resulting in significantly less than 100% quantum efficiency. Secondly, the current enhancement mechanism occurs with a much lower applied field than in the case of  $\text{SiO}_2$ . The mechanism for the current enhancement in  $\text{Al}_2\text{O}_3$  is believed to be the trapping of positive charge (holes) in the aluminum oxide film. Two possible models have been presented, one in which holes are mobile and one in which they are immobile. Either model can explain the presently observed experimental results. In either case, under irradiation the accumulation of positive charge in  $\text{Al}_2\text{O}_3$  continues until the interface field is sufficient to produce tunnel injection from the silicon. This occurs at a much lower field in  $\text{Al}_2\text{O}_3$  than in  $\text{SiO}_2$ , owing to the trap-assisted tunneling mechanism that has been described previously. Analyses of the photocurrents in this experiment have shown that it is not possible to distinguish between a model in which holes are immobile and the photocurrent results from merely the sweepout of electrons and a model in which holes are mobile and traverse the oxide. Interpretation of the results

in  $\text{Al}_2\text{O}_3$  are complicated by the presence of large electron trapping and the relatively low injection threshold for electrons. The presence of both electron and hole trapping in  $\text{Al}_2\text{O}_3$  and the difficulty in determining the location of the space charge by etching techniques make it very hard to distinguish between models involving mobile holes and immobile holes. Therefore, until some new experimental techniques are developed, it appears impossible to distinguish between the two models.

#### C. PHOTOINJECTION EXPERIMENTS

Photoinjection experiments have provided very useful information in several ways. Charge centroid measurements have shown that a large fraction of the charge injected into  $\text{Al}_2\text{O}_3$  is trapped near the injecting electrode. Comparison of the experimental data with two limiting models shows that no conclusions can be drawn regarding the spatial distribution of traps but that trapping is localized to the interface region. Similar measurements on Si-SiO<sub>2</sub>- $\text{Al}_2\text{O}_3$  structures have shown that trapping occurs in the  $\text{Al}_2\text{O}_3$  near the SiO<sub>2</sub> interface.

Measurements of the voltage dependence of photocurrents have provided important information regarding barrier energies and electron scattering in  $\text{Al}_2\text{O}_3$ . The Si- $\text{Al}_2\text{O}_3$  barrier is approximately 4.2 eV, and the electron scattering length in the  $\text{Al}_2\text{O}_3$  in the direction of the field is approximately 3 Å.

#### D. HIGH FIELD CHARGE INJECTION

Studies of high-field charge injection on  $\text{Al}_2\text{O}_3$  MOS structures, with purposely introduced SiO<sub>2</sub> films between the Si and  $\text{Al}_2\text{O}_3$ , have shown that very thin SiO<sub>2</sub> (~40 Å) actually enhances the electron injection. Thicker films of SiO<sub>2</sub> (~70 Å) can markedly reduce the electron injection for a given applied field in the  $\text{Al}_2\text{O}_3$ . Unfortunately, the SiO<sub>2</sub> layer, while reducing electron injection, increases the radiation sensitivity. Additionally, processing variables have an effect on the high-field injection process, but so far any reduction in the injection was accompanied by a corresponding reduction in hardness.

## REFERENCES

1. R. J. Powell and G. F. Derbenwick, *IEEE Trans. Nuclear Science* NS-19, 99 (1971).
2. A. G. Holmes-Siedle and I. Groombridge, *Thin Solid Films* 27, 165 (1975).
3. R. J. Powell, *J. Appl. Phys.* 46, 4557 (1975).
4. O. L. Curtis, J. R. Srour, and K. Y. Chiu, *J. Appl. Phys.* 45, 4506 (1974).
5. N. Klein, *Advances in Electronics and Electron Physics* 26, 309 (1971).
6. R. J. Powell, *IEEE Trans. Nuclear Science* NS-22, 2240 (1975).
7. D. F. Heath and P. A. Sacher, *Appl. Optics* 5, 937 (1966).
8. A. A. Ballman, et al., *Appl. Optics* 7, 1387 (1968).
9. H. R. Philipp, *J. Phys. Chem. Solids* 32, 1935 (1971).
10. R. M. Finne and D. L. Klein, *J. Electrochem Soc.* 114, 965 (1967).
11. *Handbook of Thermophysical Properties of Solid Materials*, Vol. 1, (MacMillan Co., New York, 1961).
12. T. A. Hahn and R. K. Kirby, *Thermal Expansion 1971 - AIP Conference Proceedings*.
13. O. S. Heavens, *Optical Properties of Thin Solid Films*, (Dover Publications, Inc., New York, 1965).
14. R. Williams, *Phys. Rev.* 140, A5669 (1965).
15. W. Groth and H. v. Weyssenhof, *Z. Naturforsch.* 11a, 165 (1956).
16. E. Loh, *Solid State Commun.* 2, 269 (1968).
17. A. R. Ruffa, *Phys. Stat. Sol.* 29, 605 (1968).
18. M. H. Reilly, *J. Phys. Chem. Solids* 31, 1041 (1970).
19. K. Platzöder, *Phys. Stat. Sol.* 29, K63 (1968).
20. T. H. DiStefano and D. E. Eastman, *Solid State Commun.* 9, 2259 (1971).
21. T. L. Gilbert, et al., *Phys. Rev.* B8, 5977 (1973).
22. A. J. Bennett and L. M. Roth, *J. Phys. Chem. Solids* 32, 1251 (1971).
23. G. A. D. Collins, D. W. J. Cruickshank, and A. Breeze, *J. Chem. Soc., Faraday Trans. II* 68, 1189 (1972).
24. K. L. Yip and W. B. Fowler, *Phys. Rev.* B10, 1400 (1974).
25. L. Pauling, *J. Phys. Chem.* 56, 361 (1952).
26. V. P. Prjanishnikov, et al., *Proc. IX International Congress on Glass, Versaille*, Vol. 1, pp. 119-131 (1971).
27. G. M. Bartenev, et al., *Izvestiya Akademii Nauk SSSR, Nerorganicheskie Materialy* 6, 1553 (1970).
28. A. G. Revesz, *J. Non-Crystalline Solids* 11, 309 (1973).

29. T. H. DiStefano and D. E. Eastman, Phys. Rev. Letters 27, 1560 (1971).
30. R. Williams and M. H. Woods, J. Appl. Phys. 46, 695 (1975).
31. B. E. Deal, et al., J. Electrochem. Soc. 114, 266 (1967)
32. M. H. Woods and R. Williams, to be published, J. Appl. Phys., Feb. 1976.

TRW SYSTEMS GROUP  
ATTN AARON H NAREVSKY RL-2144  
ONE SPACE PARK  
REDONDO BEACH, CA 90278

IRT CORPORATION  
ATTN K L GERTZ  
P.O. BOX 81087  
SAN DIEGO, CA 92138

LABEL 00000000AJ03LB 0007623701762

IRT CORPORATION  
ATTN LEU D COTTER  
P.O. BOX 81087  
SAN DIEGO, CA 92138

LABEL 00000000AJ03LB 0007623701762

IRT CORPORATION  
ATTN RALPH H STAHL  
P.O. BOX 81087  
SAN DIEGO, CA 92138

COPY AVAILABLE TO DDC DOES NOT  
PERMIT FULLY LEGIBLE PRODUCTION

DIRECTOR  
DEFENSE ADVANCED RESEARCH AGENCY  
ATTN STU LTC ROBERT P SULLIVAN  
ARCHITECT BUILDING  
1400 WILSON BLVD.  
ARLINGTON, VA 22209

IRT CORPORATION  
ATTN JAMES A WASEY  
P.O. BOX 81087  
SAN DIEGO, CA 92138

DEFENSE COMMUNICATION ENGINEER CENTER  
ATTN CODE R320 C W BERGMAN  
1860 NICHLE AVENUE  
RESTON, VA 22090

JOHNS HOPKINS UNIVERSITY  
ATTN PETER E FARTRIDGE  
APPLIED PHYSICS LABORATORY  
JOHNS HOPKINS ROAD  
LAUREL MD 20610

WESTINGHOUSE ELECTRIC CORPORATION  
ATTN HENRY P KALAPACA H S 3525  
DEFENSE AND ELECTRONIC SYSTEMS CTR  
P.O. BOX 1693  
FRIENDSHIP INTERNATIONAL AIRPORT  
BALTIMORE, MD 21203

KAMAN SCIENCES CORPORATION  
ATTN DONALD H BRUCE  
P.O. BOX 7443  
COLORADO SPRINGS, CO 80933

WESTINGHOUSE ELECTRIC CORPORATION  
ATTN WILLIAM E NEWELL  
RESEARCH AND DEVELOPMENT CENTER  
1310 HEULAH ROAD, CHURCHILL BOROUGH  
PITTSBURGH, PA 15235

UNITED TECHNOLOGIES CORPORATION  
ATTN RAYMOND G GIGUERE  
HAMILTON STANDARD DIVISION  
BRADLEY INTERNATIONAL AIRPORT  
WINDSOR LOCKS, CT 06099

37

CHARLES STARK DRAPER LABORATORY INC  
ATTN RICHARD G HALTMAIER  
68 ALBANY STREET  
CAMBRIDGE, MA 02139

DIKEWOOD CORPORATION, THE  
ATTN L WAYNE DAVIS  
1009 BRADBURY DRIVE, S.E.  
UNIVERSITY RESEARCH PARK  
ALBUQUERQUE, NM 87106

CHARLES STARK DRAPER LABORATORY INC  
ATTN KENNETH FERTIG  
68 ALBANY STREET  
CAMBRIDGE, MA 02139

E-SYSTEMS, INC.  
ATTN LIBRARY 8-50100  
GREENVILLE DIVISION  
P.O. BOX 1056  
GREENVILLE, TX 75401

CHARLES STARK DRAPER LABORATORY INC  
ATTN PAUL R KELLY  
68 ALBANY STREET  
CAMBRIDGE, MA 02139

EFFECTS TECHNOLOGY, INC.  
ATTN EDWARD JOHN STEELE  
5383 HOLLISTER AVENUE  
SANTA BARBARA, CA 93105

CINCINNATI ELECTRONICS CORPORATION  
ATTN C R STUMP  
2630 GLENDALE - MILFORD ROAD  
CINCINNATI, OH 45241

ELECTRONICS TECHNOLOGY LABORATORY  
ATTN R CURRY (UNCL ONLY)  
ENGINEERING EXPERIMENT STATION  
GEORGIA INSTITUTE OF TECHNOLOGY  
ATLANTA, GA 30332

CINCINNATI ELECTRONICS CORPORATION  
ATTN LOIS HAMMOND  
2630 GLENDALE - MILFORD ROAD  
CINCINNATI, OH 45241

EXP & MATH PHYSICS CONSULTANTS  
ATTN THOMAS M JORDAN  
P.O. BOX 66331  
LOS ANGELES, CA 90066

COMPUTER SCIENCES CORPORATION  
ATTN RICHARD H DICHAUT  
201 LA VETA DRIVE N.E.  
ALBUQUERQUE, NM 87106

FAIRCHILD CAMERA AND INSTRUMENT CORP  
ATTN SEC DEPT FOR 2-233 DAVID K MYERS  
464 ELLIS STREET  
MOUNTAIN VIEW, CA 94040

CUTLER-HAMMER, INC.  
ATTN CENTRAL TECH FILES ANNE ANTHONY  
AIL DIVISION  
COMAC ROAD  
DEER PARK, NY 11729

FAIRCHILD INDUSTRIES, INC.  
ATTN MGR COLLECTING DATA & STANDARDS  
SHERMAN FAIRCHILD TECHNOLOGY CENTER  
20301 CENTURY BOULEVARD  
GERMANTOWN, MD 20767

COPY AVAILABLE TO DDC DOES NOT  
PERMIT FULLY LEGIBLE PRODUCTION

SANDIA LABORATORIES  
ATTN DDC CON FOR DRG 2110 J A HOOD  
P.O. BOX 5800  
ALBUQUERQUE, NM 87115

UNIVERSITY OF CALIFORNIA  
LAWRENCE LIVERMORE LABORATORY  
ATTN DONALD J MEEKER L-545 (CLASS L-1)  
P.O. BOX 808  
LIVERMORE CA 94550

SANDIA LABORATORIES  
ATTN DDC CON FOR DRG 1933 E N COPPAGE  
P.O. BOX 5800  
ALBUQUERQUE, NM 87115

UNIVERSITY OF CALIFORNIA  
LAWRENCE LIVERMORE LABORATORY  
ATTN HANS FRUEKER L-96 (CLASS L-94)  
P.O. BOX 808  
LIVERMORE CA 94550

SANDIA LABORATORIES  
ATTN DDC CON FOR JACK V WALKER 5220  
P.O. BOX 5800  
ALBUQUERQUE, NM 87115

UNIVERSITY OF CALIFORNIA  
LAWRENCE LIVERMORE LABORATORY  
ATTN FREDERICK R KOVAP L-31 (CLASS L-1)  
P.O. BOX 808  
LIVERMORE CA 94550

SANDIA LABORATORIES  
ATTN DIV 5231 JAMES H PENKEN  
P.O. BOX 5800  
ALBUQUERQUE, NM 87115

LOS ALAMOS SCIENTIFIC LABORATORY  
ATTN DDC CON FOR MARVIN C HOFFMAN  
P.O. BOX 1663  
LOS ALAMOS, NM 87545

SANDIA LABORATORIES  
ATTN DDC CON FOR 3141 SANDIA RPT COL  
P.O. BOX 5800  
ALBUQUERQUE, NM 87115

LOS ALAMOS SCIENTIFIC LABORATORY  
ATTN DDC CON FOR J ARTHUR FREED  
P.O. BOX 1663  
LOS ALAMOS, NM 87545

U S ENERGY RSCH & DEV ADMIN  
ATTN DOCUMENT CONTROL FOR WSSR  
ALBUQUERQUE OPERATIONS OFFICE  
P.O. BOX 5400  
ALBUQUERQUE, NM 87115

LOS ALAMOS SCIENTIFIC LABORATORY  
ATTN DDC CON FOR BRUCE W NOEL  
P.O. BOX 1663  
LOS ALAMOS, NM 87545

CENTRAL INTELLIGENCE AGENCY  
ATTN ALICE A PADGETT  
ATTN: RO/SI RM 5G48 HQ BLDG  
WASHINGTON, DC 20505

SANDIA LABORATORIES  
ATTN DDC CON FOR THEODORE A BELLIN  
LIVERMORE LABORATORY  
P.O. BOX 969  
LIVERMORE, CA 94550

COPY AVAILABLE TO DDC DOES NOT  
PERMIT FULLY LEGIBLE PRODUCTION

SAMS0/DY  
ATTN DYS MAJ LARRY A DARDA  
POST OFFICE BOX 92960  
WORLDWAY POSTAL CENTER  
LOS ANGELES, CA 90009  
(TECHNOLOGY)

SAMS0/DY  
ATTN DYS CAPT WAYNE SCHORER  
POST OFFICE BOX 92960  
WORLDWAY POSTAL CENTER  
LOS ANGELES, CA 90009  
(TECHNOLOGY)

SAMS0/IN  
ATTN IND I J JUDY  
POST OFFICE BOX 92960  
WORLDWAY POSTAL CENTER  
LOS ANGELES, CA 90009  
(INTELLIGENCE)

SAMS0/MN  
ATTN MNNG CAPT DAVID J STORREL  
NORTON AFB, CA 92400  
(MINUTEMAN)

SAMS0/RS  
ATTN RSSE LTC KENNETH L GILBERT  
POST OFFICE BOX 92960  
WORLDWAY POSTAL CENTER  
LOS ANGELES, CA 90009  
(REENTRY SYSTEMS)

SAMS0/RS  
ATTN RSE  
POST OFFICE BOX 92960  
WORLDWAY POSTAL CENTER  
LOS ANGELES, CA 90009  
(REENTRY SYSTEMS)

SAMS0/SZ  
ATTN SZJ CAPT JOHN H SALCH  
POST OFFICE BOX 92960  
WORLDWAY POSTAL CENTER  
LOS ANGELES, CA 90009  
(SPACE DEFENSE SYSTEMS)

SAMS0/YD  
ATTN YDD MAJ HARION F SCHNEIDER  
POST OFFICE BOX 92960  
WORLDWAY POSTAL CENTER  
LOS ANGELES, CA 90009

(DEF METEOROLOGICAL SAT SYS)

COMMANDER IN CHIEF  
STRATEGIC AIR COMMAND  
ATTN NFI-STINFO LIBRARY  
OFFUTT AFB, NE 68113

COMMANDER IN CHIEF  
STRATEGIC AIR COMMAND  
ATTN XPF5 MAJ BRIAN G STEPHAN  
OFFUTT AFB, NE 68113

UNIVERSITY OF CALIFORNIA  
LAWRENCE LIVERMORE LABORATORY  
ATTN JOSEPH F KELLER JP L-125  
P.O. BOX 808  
LIVERMORE CA 94550

UNIVERSITY OF CALIFORNIA  
LAWRENCE LIVERMORE LABORATORY  
ATTN LAWRENCE CLELAND L-156  
P.O. BOX 808  
LIVERMORE CA 94550

UNIVERSITY OF CALIFORNIA  
LAWRENCE LIVERMORE LABORATORY  
ATTN RONALD L OTT L-531  
P.O. BOX 808  
LIVERMORE CA 94550

UNIVERSITY OF CALIFORNIA  
LAWRENCE LIVERMORE LABORATORY  
ATTN TECH INFO DEPT L-3  
P.O. BOX 808  
LIVERMORE CA 94550

COPY AVAILABLE TO DDC DOES NOT  
PERMIT FULLY LEGIBLE PRODUCTION

DIRECTOR  
STRATEGIC SYSTEMS PROJECT OFFICE  
ATTN NSP-27331 PHIL SPECTOR  
NAVY DEPARTMENT  
WASHINGTON, DC 20376

AF WEAPONS LABORATORY, AFSC  
ATTN ELA  
KIRTLAND AFB, NM 87117

DIRECTOR  
STRATEGIC SYSTEMS PROJECT OFFICE  
ATTN NSP-2342 RICHARD L COLEMAN  
NAVY DEPARTMENT  
WASHINGTON, DC 20376

AF WEAPONS LABORATORY, AFSC  
ATTN SAT  
KIRTLAND AFB, NM 87117

AF GEOPHYSICS LABORATORY, AFSC  
ATTN L33-STOP 30 FREEMAN SHEPHERD  
HANSCOM AFB, MA 01731

AF WEAPONS LABORATORY, AFSC  
ATTN SAB  
KIRTLAND AFB, NM 87117

AF GEOPHYSICS LABORATORY, AFSC  
ATTN EMERY CORMIER  
HANSCOM AFB, MA 01731

AFYAC  
ATTN TAE  
PATRICK AFB, FL 32925

AF GEOPHYSICS LABORATORY, AFSC  
ATTN LIA EDWARD A BURKE  
HANSCOM AFB, MA 01731

HEADQUARTERS  
ELECTRONIC SYSTEMS DIVISION, (AFSC)  
ATTN YSE, LTC DAVID C SPARKS  
L. G. HANSCOM FIELD  
REDFORD, MA 01730

AF INSTITUTE OF TECHNOLOGY, AIJ  
ATTN ENP CHARLES J BRIDGMAN  
WRIGHT-PATTERSON AFB, OH 45433

COMMANDER  
FOREIGN TECHNOLOGY DIVISION, AFSC  
ATTN ETET CAPT RICHARD C HULSEMAN  
WRIGHT-PATTERSON AFB, OH 45433

AF MATERIALS LABORATORY, AFSC  
ATTN LTE  
WRIGHT-PATTERSON AFB, OH 45433

COMMANDER  
ROME AIR DEVELOPMENT CENTER, AFSC  
ATTN RBRAC 1 L KRULAC  
GRIFFISS AFB, NY 13440

COPY AVAILABLE TO DDC DOES NOT  
PERMIT FULLY LEGIBLE PRODUCTION

AERONUTRONIC FORD CORPORATION  
ATTN EDWARD R HAHN MS-422  
WESTERN DEVELOPMENT LABORATORIES DIV  
3939 FABIAN WAY  
PALO ALTO, CA 94303

COMMANDER  
NAVAL SURFACE WEAPONS CENTER  
ATTN WILLIAM H HOLT  
DAHLGREN LABORATORY  
DAHLGREN, VA 22448

AERONUTRONIC FORD CORPORATION  
ATTN DONALD R MCMORRO, MS 630  
WESTERN DEVELOPMENT LABORATORIES DIV  
3939 FABIAN WAY  
PALO ALTO, CA 94303

COMMANDER  
NAVAL WEAPONS CENTER  
ATTN CODE 533 TECH LIB  
CHINA LAKE, CA 93555

AEROSPACE CORPORATION  
ATTN WILLIAM A WILLIS  
P.O. BOX 92957  
LOS ANGELES, CA 90009

COMMANDING OFFICER  
NAVAL WEAPONS EVALUATION FACILITY  
ATTN CODE ATG MR STANLEY  
WRIGHTLAND AIR FORCE BASE  
ALBUQUERQUE, NM 87117

AEROSPACE CORPORATION  
ATTN MELVIN I BERNSTEIN  
P.O. BOX 92957  
LOS ANGELES, CA 90009

COMMANDING OFFICER  
NAVAL WEAPONS SUPPORT CENTER  
ATTN CODE 70242 JOSEPH A MURARIN  
CRANE, IN 47522

AEROSPACE CORPORATION  
ATTN IRVING M GARFUNKEL  
P.O. BOX 92957  
LOS ANGELES, CA 90009

COMMANDING OFFICER  
NAVAL WEAPONS SUPPORT CENTER  
ATTN CODE 7024 JAMES RAMSEY  
CRANE, IN 47522

AEROSPACE CORPORATION  
ATTN JULIAN REINHEIMER  
P.O. BOX 92957  
LOS ANGELES, CA 90009

COMMANDING OFFICER  
NUCLEAR WEAPONS TNG CENTER PACIFIC  
ATTN CODE 50  
NAVAL AIR STATION, NORTH ISLAND  
SAN DIEGO, CA 92135

AEROSPACE CORPORATION  
ATTN L W AUERMAN  
P.O. BOX 92957  
LOS ANGELES, CA 90009

DIRECTOR  
STRATEGIC SYSTEMS PROJECT OFFICE  
ATTN SP 2701 JOHN W PITSEMBERGER  
NAVY DEPARTMENT  
WASHINGTON, DC 20374

COPY AVAILABLE TO DDC DOES NOT  
PERMIT FULLY LEGIBLE PRODUCTION

DEPARTMENT OF COMMERCE  
ATTN APPL RAD DIV ROBERT C PLACIUS  
NATIONAL BUREAU OF STANDARDS  
WASHINGTON, DC 20234

CHIEF OF NAVAL RESEARCH  
ATTN CODE 421 DORAN & PADGETT  
NAVY DEPARTMENT  
ARLINGTON, VA 22217

DEPARTMENT OF COMMERCE  
ATTN JUDSON C FRENCH  
NATIONAL BUREAU OF STANDARDS  
WASHINGTON, DC 20234

COMMANDER  
NAVAL ELECTRONIC SYSTEMS COMMAND  
ATTN ELEX 05323 CLEVELAND F WATKINS  
NAVAL ELECTRONIC SYSTEMS CMD HQS  
WASHINGTON, DC 20360

AEROJET ELECTRO-SYSTEMS CO DIV  
ATTN THOMAS D HANSON  
AEROJET-GENERAL CORPORATION  
P.O. BOX 296  
AZUSA, CA 91702

COMMANDER  
NAVAL ELECTRONIC SYSTEMS COMMAND  
ATTN CODE 5032 CHARLES J WELLS  
NAVAL ELECTRONIC SYSTEMS CMD HQS  
WASHINGTON, DC 20360

AERONUTRONIC FORD CORPORATION  
ATTN E M PONCELET JR  
AEROSPACE & COMMUNICATIONS OPS  
AERONUTRONIC DIVISION  
FORD & JAMBOREE ROADS

COMMANDER  
NAVAL ELECTRONIC SYSTEMS COMMAND  
ATTN CODE 504510  
NAVAL ELECTRONIC SYSTEMS CMD HQS  
WASHINGTON, DC 20360

NEWPORT BEACH, CA 92663

AERONUTRONIC FORD CORPORATION  
ATTN KEN C ATTINGER  
AEROSPACE & COMMUNICATIONS OPS  
AERONUTRONIC DIVISION  
FORD & JAMBOREE ROADS  
NEWPORT BEACH, CA 92663

COMMANDER  
NAVAL ELECTRONIC SYSTEMS COMMAND  
  
ATTN PME 117-21  
NAVAL ELECTRONIC SYSTEMS CMD HQS  
WASHINGTON, DC 20360

AERONUTRONIC FORD CORPORATION  
ATTN TECH INFO SECTION  
AEROSPACE & COMMUNICATIONS OPS  
AERONUTRONIC DIVISION  
FORD & JAMBOREE ROADS  
NEWPORT BEACH, CA 92663

COMMANDING OFFICER  
NAVAL INTELLIGENCE SUPPORT CTR  
ATTN P ALEXANDER  
4301 SUITLAND ROAD BLDG. 5  
WASHINGTON, DC 20390

AERONUTRONIC FORD CORPORATION  
ATTN SAMUEL R CRA FORD MS 531  
WESTERN DEVELOPMENT LABORATORIES DIV  
3939 FABIAN WAY  
PALO ALTO, CA 94303

COMMANDING OFFICER  
NAVAL INTELLIGENCE SUPPORT CTR  
ATTN NISC-45  
4301 SUITLAND ROAD BLDG. 5  
WASHINGTON, DC 20390

COPY AVAILABLE TO DDC DOES NOT  
PERMIT FULLY LEGIBLE PRODUCTION

COMMANDER  
U S ARMY MOBILITY EQUIP R&D CTR  
ATTN STSFB-MW JOHN W BOND JR  
FORT BELVOIR, VA 22060

COMMANDER  
U S ARMY MATERIEL DEV & READINESS CMD  
ATTN DRUDE-D LAWRENCE FLYNN  
5001 EISENHOWER AVENUE  
ALEXANDRIA, VA 22333

CHIEF  
U S ARMY NUC AND CHEMICAL SURETY GP  
ATTN MUSG-ND MAJ SIDNEY W WINSLOW  
BLDG. 2073, NORTH AREA  
FT. BELVOIR, VA 22060

COMMANDER  
U S ARMY MISSILE COMMAND  
ATTN DRSMI-RGD VIC RUWE (UNCL ONLY)  
REDSTONE ARSENAL, AL 35899

COMMANDER  
U S ARMY NUCLEAR AGENCY  
ATTN ATCN- LTC LEONARD A SLUGA  
FORT BLISS, TX 79916

COMMANDER  
U S ARMY MISSILE COMMAND  
ATTN DRCPM-MOTI CPT JEFF A SIMS  
REDSTONE ARSENAL, AL 35899

COMMANDER  
U S ARMY TEST AND EVALUATION COMD  
ATTN DRSTE-EL RICHARD Y KOLCHIN  
ABERDEEN PROVING GROUND, MD 21005

COMMANDER  
U S ARMY MISSILE COMMAND  
ATTN DRCPM-LCEX HOWARD H HENRIKSEN  
REDSTONE ARSENAL, AL 35899

COMMANDER  
U S ARMY TEST AND EVALUATION COMD  
ATTN DRSTE-NB RUSSELL R GALASSO  
ABERDEEN PROVING GROUND, MD 21005

COMMANDER  
U S ARMY MISSILE COMMAND  
ATTN DRSMI-RGP HUGH GREEN  
REDSTONE ARSENAL, AL 35899

COMMANDER  
WHITE SANDS MISSILE RANGE  
ATTN STEAS-TE-NT MARVIN P SQUIRES  
WHITE SANDS MISSILE RANGE, N. 88002

COMMANDER  
U S ARMY MISSILE COMMAND  
ATTN DRSMI-RRH FAISON P GIBSON  
REDSTONE ARSENAL, AL 35899

CHIEF OF NAVAL RESEARCH  
ATTN CODE 427  
NAVY DEPARTMENT  
ARLINGTON, VA 22217

COMMANDER  
U S ARMY MISSILE COMMAND  
ATTN DRCPM-PE-EA WALLACE G WAGNER  
REDSTONE ARSENAL, AL 35899

COPY AVAILABLE TO DDG DOES NOT  
PERMIT FULLY LEGIBLE PRODUCTION

COMMANDER  
U S ARMY ELECTRONICS COMMAND  
ATTN DRSEL-CT-HDX ABRAHAM F COHEN  
FORT MONMOUTH, NJ 07703

DIRECTOR  
U S ARMY BALLISTIC RESEARCH LABS  
ATTN DRXRR-X JULIUS J MESZAROS  
ABERDEEN PROVING GROUND, MD 21005

COMMANDER  
U S ARMY ELECTRONICS COMMAND  
ATTN DRSEL-GG-TD W R WERK (NO CNDWI)  
FORT MONMOUTH, NJ 07703

DIRECTOR  
U S ARMY BALLISTIC RESEARCH LABS  
ATTN DRABK-VL ROBERT L HARRISON  
ABERDEEN PROVING GROUND, MD 21005

COMMANDER  
U S ARMY ELECTRONICS COMMAND  
ATTN DRSEL-TL-EN ROBERT LUY  
FORT MONMOUTH, NJ 07703

DIRECTOR  
U S ARMY BALLISTIC RESEARCH LABS  
ATTN DRXRR-AM W R VANANTWERP  
ABERDEEN PROVING GROUND, MD 21005

COMMANDER  
U S ARMY ELECTRONICS COMMAND  
ATTN DRSEL-TL-TO GERHART J GAULE  
FORT MONMOUTH, NJ 07703

DIRECTOR  
U S ARMY BALLISTIC RESEARCH LABS  
ATTN DRARD-RVL DAVID L RIGATTI  
ABERDEEN PROVING GROUND, MD 21005

COMMANDER  
U S ARMY ELECTRONICS COMMAND  
ATTN DRSEL-TL-ND S W POPENREY  
FORT MONMOUTH, NJ 07703

CHIEF  
U S ARMY COMMUNICATIONS SYS AGENCY  
ATTN SCCM-AU-SV LIBRARY  
FORT MONMOUTH, NJ 07703

COMMANDER  
U S ARMY ELECTRONICS COMMAND  
ATTN DRSEL-PL-ENV HANS A BOMKE  
FORT MONMOUTH, NJ 07703

COMMANDER  
U S ARMY ELECTRONICS COMMAND  
ATTN DRSEL-TL-EN E ROTH  
FORT MONMOUTH, NJ 07703

COMMANDER-IN-CHIEF  
U S ARMY EUROPE AND SEVENTH ARMY  
ATTN ODCSE-E AEAGE-PI  
APO NEW YORK 09403

COMMANDER  
U S ARMY ELECTRONICS COMMAND  
ATTN DRSEL-TL-IR EDWIN T HUNTER  
FORT MONMOUTH, NJ 07703

COPY AVAILABLE TO DDC DOES NOT  
PERMIT FULLY LEGIBLE PRODUCTION

COMMANDER  
PICATINNY ARSENAL  
ATTN SMUPA-TN BURTON V FRANKS  
DOVER, NJ 07801

COMMANDER  
HARRY DIAMOND LABORATORIES  
ATTN DRADO-TI TECH LTR  
2800 POWDER MILL ROAD  
ADELPHI MD 20783

COMMANDER  
PICATINNY ARSENAL  
ATTN SARPA-ND-C-E AMINA NORDIN  
DOVER, NJ 07801

COMMANDING OFFICER  
NIGHT VISION LABORATORY  
ATTN CAPT ALLAN S PARKER  
U S ARMY ELECTRONICS COMMAND  
FORT BELVOIR, VA 22060

COMMANDER  
PICATINNY ARSENAL  
ATTN SARPA-ND-N  
DOVER, NJ 07801

COMMANDER  
PICATINNY ARSENAL  
ATTN SMUPA-FR-S-P  
DOVER, NJ 07801

COMMANDER  
REDSTONE SCIENTIFIC INFORMATION CTR  
ATTN CHIEF, DOCUMENTS  
U.S. ARMY MISSILE COMMAND  
REDSTONE ARSENAL AL 35809

COMMANDER  
PICATINNY ARSENAL  
ATTN SARPA-FR-E LOUIS A. BERTI  
DOVER, NJ 07801

SECRETARY OF THE ARMY  
ATTN ODUSA DR DANIEL WILLARD  
WASHINGTON, DC 20310

COMMANDER  
PICATINNY ARSENAL  
ATTN SMUPA-ND-W  
DOVER, NJ 07801

COMMANDER  
TRASANA  
ATTN ATAA-EAC FRANCIS N. INANS  
WHITE SANDS MISSILE RANGE NM 88002

COMMANDER  
PICATINNY ARSENAL  
ATTN SMUPA-ND-N-E  
DOVER, NJ 07801

DIRECTOR  
U S ARMY BALLISTIC RESEARCH LABS  
ATTN DR YBR-VL JOHN W KINCH  
ABERDEEN PROVING GROUND, MD 21005

COMMANDER  
PICATINNY ARSENAL  
ATTN SMUPA-ND-D-R EDWARD J ARBER  
DOVER, NJ 07801

COPY AVAILABLE TO DDC DOES NOT  
PERMIT FULLY LEGIBLE PRODUCTION

COMMANDER  
HARRY DIAMOND LABORATORIES  
ATTN DRXDD-RCC JOHN A ROSANO  
2800 POWDER MILL ROAD  
ADELPHI MD 20783

DIRECTOR  
NATIONAL SECURITY AGENCY  
ATTN TBL  
FT. GEORGE G. MEADE MD 20755

COMMANDER  
HARRY DIAMOND LABORATORIES  
ATTN DRXDD-NP FRANCIS N WIMENITZ  
2800 POWDER MILL ROAD  
ADELPHI MD 20783

PROJECT MANAGER  
ARMY TACTICAL DATA SYSTEMS  
ATTN DRXDD-TDS-SD  
U S ARMY ELECTRONICS COMMAND  
FORT MONMOUTH NJ 07703

COMMANDER  
HARRY DIAMOND LABORATORIES  
ATTN DRXDD-RA JOSEPH P MILETTA  
2800 POWDER MILL ROAD  
ADELPHI MD 20783

PROJECT MANAGER  
ARMY TACTICAL DATA SYSTEMS  
ATTN CLAINF R HOFF E  
U S ARMY ELECTRONICS COMMAND  
FORT MONMOUTH NJ 07703

COMMANDER  
HARRY DIAMOND LABORATORIES  
ATTN DRXDD-RCC JOHN E THOMPkins  
2800 POWDER MILL ROAD  
ADELPHI MD 20783

COMMANDER  
RMD SYSTEMS COMMAND  
ATTN UNSC-TEL NOAH J HIRST  
P.O. BOX 150  
HUNTSVILLE AL 35807

COMMANDER  
HARRY DIAMOND LABORATORIES  
ATTN DRXDD-EM R BUSTAK  
2800 POWDER MILL ROAD  
ADELPHI MD 20783

COMMANDER  
FRANKFORD ARSENAL  
ATTN SAKFA-FCU MARVIN FLECKER  
BRIDGE AND TALONY STREETS  
PHILADELPHIA PA 19137

COMMANDER  
HARRY DIAMOND LABORATORIES  
ATTN DRXDD-RBH PAUL A CALDWELL  
2800 POWDER MILL ROAD  
ADELPHI MD 20783

COMMANDER  
HARRY DIAMOND LABORATORIES  
ATTN DRXDD-RC ROBERT B OSWALD JR  
2800 POWDER MILL ROAD  
ADELPHI MD 20783

COMMANDER  
HARRY DIAMOND LABORATORIES  
ATTN DRXDD-RB ROBERT E MCCOSKEY  
2800 POWDER MILL ROAD  
ADELPHI MD 20783

COMMANDER  
HARRY DIAMOND LABORATORIES  
ATTN DRXDD-TR EDWARD E CONRAD  
2800 POWDER MILL ROAD  
ADELPHI MD 20783

COPY AVAILABLE TO DDC DOES NOT  
PERMIT FULLY LEGIBLE PRODUCTION

DIRECTOR  
DEFENSE COMMUNICATIONS AGENCY  
ATTN CODE 930 MONTE I BURGESS JR  
WASHINGTON, DC 20305

DIRECTOR  
DEFENSE NUCLEAR AGENCY  
ATTN STVL  
WASHINGTON, DC 20305

DEFENSE DOCUMENTATION CENTER  
ATTN T  
CAMERON STATION  
ALEXANDRIA, VA 22314

COMMANDER  
FIELD COMMAND  
ATTN FCPR  
DEFENSE NUCLEAR AGENCY  
KIRTLAND AFB, NM 87115

DIRECTOR  
DEFENSE INTELLIGENCE AGENCY  
ATTN DS-442  
WASHINGTON, DC 20301

DIRECTOR  
INTERSERVICE NUCLEAR WEAPONS SCHOOL  
ATTN DOCUMENT CONTROL  
KIRTLAND AFB, NM 87115

DIRECTOR  
DEFENSE NUCLEAR AGENCY  
ATTN 04TN  
WASHINGTON, DC 20305

DIRECTOR  
JOINT STRAT TGT PLANNING STAFF JCS  
ATTN JLT4-2  
OFFUTT AFB  
OMAHA, NE 68113

DIRECTOR  
~~DEFENSE NUCLEAR AGENCY~~  
ATTN STVL TECH LIBRARY  
WASHINGTON, DC 20305

CHIEF  
LIVERMORE DIVISION FLD COMMAND DNA  
ATTN DOCUMENT CONTROL FOR L-395  
LAWRENCE LIVERMORE LABORATORY  
P.O. BOX 808  
LIVERMORE, CA 94550

DIRECTOR  
DEFENSE NUCLEAR AGENCY  
ATTN 00ST  
WASHINGTON, DC 20305

CHIEF  
LIVERMORE DIVISION FLD COMMAND DNA  
ATTN FCPR  
LAWRENCE LIVERMORE LABORATORY  
P.O. BOX 808  
LIVERMORE, CA 94550

DIRECTOR  
DEFENSE NUCLEAR AGENCY  
ATTN RAEV  
WASHINGTON, DC 20305

DIRECTOR  
NATIONAL SECURITY AGENCY  
ATTN ORLAND O VAN GUNTEN R-425  
FT. GEORGE G. MEADE, MD 20755

COPY AVAILABLE TO DDC DOES NOT  
PERMIT FULLY LEGIBLE PRODUCTION

TRW SYSTEMS GROUP  
ATTN PAUL HOLMUD RI-1196  
ONE SPACE PARK  
REDONDO BEACH, CA 90278

TEXAS TECH UNIVERSITY  
ATTN TRAVIS L SIMPSON  
P.O. BOX 5404 NORTH COLLEGE STATION  
LURROCK, TX 79417

TRW SYSTEMS GROUP  
ATTN LILLIAN D SINGLETON RI, 1070  
ONE SPACE PARK  
REDONDO BEACH, CA 90278

TRW SYSTEMS GROUP  
ATTN ALLAN ANDERMAN RI-1132  
ONE SPACE PARK  
REDONDO BEACH, CA 90278

TRW SYSTEMS GROUP  
ATTN R D LOFLAND RI-1028  
ONE SPACE PARK  
REDONDO BEACH, CA 90278

TRW SYSTEMS GROUP  
ATTN A A LITTLE MS RI-1120  
ONE SPACE PARK  
REDONDO BEACH, CA 90278

TRW SYSTEMS GROUP  
ATTN RICHARD H KINGSLAND RI-2154  
ONE SPACE PARK  
REDONDO BEACH, CA 90278

TRW SYSTEMS GROUP  
ATTN A D LIERSCHUTZ RI-1162  
ONE SPACE PARK  
REDONDO BEACH, CA 90278

TRW SYSTEMS GROUP  
ATTN H S JENSEN  
SAN BERNARDINO OPERATIONS  
P.O. BOX 1310  
SAN BERNARDINO, CA 92402

TRW SYSTEMS GROUP  
ATTN TECH INFO CENTER/S-1930  
ONE SPACE PARK  
REDONDO BEACH, CA 90278

TRW SYSTEMS GROUP  
ATTN JOHN F DANKS  
SAN BERNARDINO OPERATIONS  
P.O. BOX 1310  
SAN BERNARDINO, CA 92402

TRW SYSTEMS GROUP  
ATTN WILLIAM H ROBINETTE JR  
ONE SPACE PARK  
REDONDO BEACH, CA 90278

TRW SYSTEMS GROUP  
ATTN EARL S ALLEN  
SAN BERNARDINO OPERATIONS  
P.O. BOX 1310  
SAN BERNARDINO, CA 92402

TRW SYSTEMS GROUP  
ATTN JERRY I LOHELL  
ONE SPACE PARK  
REDONDO BEACH, CA 90278

COPY AVAILABLE TO DDC DOES NOT  
PERMIT FULLY LEGIBLE PRODUCTION

DIRECTOR  
NAVAL RESEARCH LABORATORY  
ATTN CODE 6631 JAMES C RITTER  
WASHINGTON, DC 20375

COMMANDER  
NAVAL SEA SYSTEMS COMMAND  
ATTN SEA-9931 SAMUEL A BARRAM  
NAVY DEPARTMENT  
WASHINGTON DC 20362

DIRECTOR  
NAVAL RESEARCH LABORATORY  
ATTN CODE 4004 EMANUEL L BRANCATO  
WASHINGTON, DC 20375

COMMANDER  
NAVAL SEA SYSTEMS COMMAND  
ATTN SEA-9931 RILEY B LANE  
NAVY DEPARTMENT  
WASHINGTON DC 20362

DIRECTOR  
NAVAL RESEARCH LABORATORY  
ATTN CODE 7701 JACK D BROWN  
WASHINGTON, DC 20375

COMMANDER  
NAVAL SHIP ENGINEERING CENTER  
ATTN CODE 517402 EDWARD F DUFFY  
CENTER BUILDING  
HYATTSVILLE, MD 20782

DIRECTOR  
NAVAL RESEARCH LABORATORY  
ATTN CODE 5216 HAROLD L HUGHES  
WASHINGTON, DC 20375

COMMANDER  
NAVAL SURFACE WEAPONS CENTER  
ATTN CODE 44501 NAVY MOC PRGMS OFF  
WHITE OAK, SILVER SPRING, MD 20910

DIRECTOR  
NAVAL RESEARCH LABORATORY  
ATTN CODE 4601 E WOLICKI  
WASHINGTON, DC 20375

COMMANDER  
NAVAL SURFACE WEAPONS CENTER  
ATTN CODE 431 EDWIN R DEAN  
WHITE OAK, SILVER SPRING, MD 20910

DIRECTOR  
NAVAL RESEARCH LABORATORY  
ATTN CODE 5210 JOHN E DAVEY  
WASHINGTON, DC 20375

COMMANDER  
NAVAL SURFACE WEAPONS CENTER  
ATTN CODE 4450 JOHN H MALLON  
WHITE OAK, SILVER SPRING, MD 20910

DIRECTOR  
NAVAL RESEARCH LABORATORY  
ATTN CODE 2627 DORIS H FOLEN  
WASHINGTON, DC 20375

COMMANDER  
NAVAL SURFACE WEAPONS CENTER  
ATTN CODE WX21 TECH LIA  
WHITE OAK, SILVER SPRING, MD 20910

COPY AVAILABLE TO DDC DOES NOT  
PERMIT FULLY LEGIBLE PRODUCTION

BOEING COMPANY, THE  
ATTN AEROSPACE LIBRARY  
P.O. BOX 3717  
SEATTLE, WA 98124

AEROSPACE CORPORATION  
ATTN LIBRARY  
P.O. BOX 92257  
LOS ANGELES, CA 90009

BOEING COMPANY, THE  
ATTN DAVID L OYE MS 87-75  
P.O. BOX 3717  
SEATTLE, WA 98124

ANALOG TECHNOLOGY CORPORATION  
ATTN JOHN JOSEPH BAHM  
3410 EAST FOOTHILL BOULEVARD  
PASADENA, CA 91107

BOEING COMPANY, THE  
ATTN HOWARD W WICKLEIN MS 17-11  
P.O. BOX 3717  
SEATTLE, WA 98124

AVCO RESEARCH & SYSTEMS GROUP  
ATTN RESEARCH LIB 4830 24 7211  
201 LOWELL STREET  
WILMINGTON, DE 19837

BOEING COMPANY, THE  
ATTN ROBERT S CALDWELL 24,00  
P.O. BOX 3717  
SEATTLE, WA 98124

BOON CORPORATION THE  
ATTN T H NEIGHBORS  
P O BOX 9274  
ALBUQUERQUE INTERNATIONAL  
ALBUQUERQUE NM 87119

RODZ-ALLEN AND HAMILTON, INC.  
ATTN RAYMOND J CHRISNER  
106 APPLE STREET  
NEW SHREWSBURY, NJ 07724

BENDIX CORPORATION, THE  
ATTN DOCUMENT CONTROL  
COMMUNICATION DIVISION  
EAST JOPPA ROAD - TOWSON  
BALTIMORE, MD 21204

CALIFORNIA INSTITUTE OF TECHNOLOGY  
ATTN A J STANLEY  
JET PROPULSION LABORATORY  
4800 OAK PARK GROVE  
PASADENA, CA 91103

BENDIX CORPORATION, THE  
ATTN MAX FRANK  
RESEARCH LABORATORIES DIVISION  
BENDIX CENTER  
SOUTHFIELD, MI 48076

CALIFORNIA INSTITUTE OF TECHNOLOGY  
ATTN J BRYDEN  
JET PROPULSION LABORATORY  
4800 OAK PARK GROVE  
PASADENA, CA 91103

BENDIX CORPORATION, THE  
ATTN MGR PRGM DEV DONALD J NIEHAUS  
RESEARCH LABORATORIES DIVISION  
BENDIX CENTER  
SOUTHFIELD, MI 48076

COPY AVAILABLE TO DDC DOES NOT  
PERMIT FULLY LEGIBLE PRODUCTION

FLORIDA UNIVERSITY OF  
ATTN D P KENNEDY  
231 AEROSPACE BLDG  
GAINESVILLE FL 32611

FRANKLIN INSTITUTE, THE  
ATTN MARIE H THOMPSON  
20TH STREET AND PARKWAY  
PHILADELPHIA PA 19103

GARRETT CORPORATION  
ATTN ROBERT F HEIR DEPT 93-9  
P.O. BOX 92240  
LOS ANGELES CA 90009

GENERAL DYNAMICS CORP.  
ATTN D J COLEMAN  
ELECTRONICS DIV ORLANDO OPERATIONS  
P.O. BOX 2566  
ORLANDO FL 32302

GENERAL ELECTRIC COMPANY  
ATTN JOHN L ANDREWS  
SPACE DIVISION  
VALLEY FORGE SPACE CENTER  
GODDARD BLVD KING OF PRUSSIA  
P.O. BOX 8555  
PHILADELPHIA PA 19101

GENERAL ELECTRIC COMPANY  
ATTN JOSEPH C PEDEN CCF 8301  
SPACE DIVISION  
VALLEY FORGE SPACE CENTER  
GODDARD BLVD KING OF PRUSSIA  
P.O. BOX 8555  
PHILADELPHIA PA 19101

GENERAL ELECTRIC COMPANY  
ATTN LARRY I CHASEN  
SPACE DIVISION  
VALLEY FORGE SPACE CENTER  
GODDARD BLVD KING OF PRUSSIA  
P.O. BOX 8555

GENERAL ELECTRIC COMPANY  
ATTN JAMES P SPRATT  
SPACE DIVISION  
VALLEY FORGE SPACE CENTER  
GODDARD BLVD KING OF PRUSSIA  
P.O. BOX 8555  
PHILADELPHIA PA 19101

GENERAL ELECTRIC COMPANY  
ATTN JOHN W PALCHOFFSKY JR  
RE-ENTRY & ENVIRONMENTAL SYSTEMS DIV  
P.O. BOX 7722  
3198 CHESTNUT STREET  
PHILADELPHIA PA 19101

GENERAL ELECTRIC COMPANY  
ATTN ROBERT A BENEDICT  
RE-ENTRY & ENVIRONMENTAL SYSTEMS DIV  
P.O. BOX 7722  
3198 CHESTNUT STREET  
PHILADELPHIA PA 19101

GENERAL ELECTRIC COMPANY  
ATTN JOSEPH J REIDL  
ORDNANCE SYSTEMS  
100 PLASTICS AVENUE  
PITTSFIELD MA 01201

GENERAL ELECTRIC COMPANY  
ATTN DASIAA  
TEMPO-CENTER FOR ADVANCED STUDIES  
816 STATE STREET (P.O. DRAWER 90)  
SANTA BARBARA CA 93102

GENERAL ELECTRIC COMPANY  
ATTN ROYDEN R RUTHERFORD  
TEMPO-CENTER FOR ADVANCED STUDIES  
816 STATE STREET (P.O. DRAWER QQ)  
SANTA BARBARA CA 93102

GENERAL ELECTRIC COMPANY  
ATTN M ESOTG  
TEMPO-CENTER FOR ADVANCED STUDIES  
816 STATE STREET (P.O. DRAWER QQ)  
SANTA BARBARA CA 93102

COPY AVAILABLE TO DDC DOES NOT  
PERMIT FULLY LEGIBLE PRODUCTION

GENERAL ELECTRIC COMPANY  
ATTN CSP 0-7 L H DEE  
P.O. BOX 1122  
SYRACUSE, NY 13201

GENERAL RESEARCH CORPORATION  
ATTN DAVID K USTAS  
WASHINGTON OPERATIONS  
WESTGATE RESEARCH PARK  
7655 OLD SPRINGHOUSE ROAD, SUITE 700  
MCLEAN, VA 22101

GENERAL ELECTRIC COMPANY  
ATTN JOHN A ELLERHORST E 2  
AIRCRAFT ENGINE GROUP  
EVENDALE PLANT  
CINCINNATI, OH 45215

GRUMMAN AEROSPACE CORPORATION  
ATTN JERRY ROGERS DEPT 533  
SOUTH OYSTER BAY ROAD  
BETHPAGE, NY 11714

GENERAL ELECTRIC COMPANY  
ATTN W J PATTERSON DROP 233  
AEROSPACE ELECTRONICS SYSTEMS  
FRENCH ROAD  
UTICA, NY 13503

GTE SYLVANIA, INC.  
ATTN LEONARD L BLAISDELL  
ELECTRONICS SYSTEMS GRP-EASTERN DIV  
77 A STREET  
NEEDHAM, MA 02194

GENERAL ELECTRIC COMPANY  
ATTN CHARLES H HEWISON DROP 624  
AEROSPACE ELECTRONICS SYSTEMS  
FRENCH ROAD  
UTICA, NY 13503

GTE SYLVANIA, INC.  
ATTN CHARLES H THORNHILL LIBRARIAN  
ELECTRONICS SYSTEMS GRP-EASTERN DIV  
77 A STREET  
NEEDHAM, MA 02194

GENERAL ELECTRIC COMPANY  
ATTN DAVID H PERIN DROP 150  
P.O. BOX 5000  
BINGHAMTON, NY 13902

GTE SYLVANIA, INC.  
ATTN JAMES A WALDON  
ELECTRONICS SYSTEMS GRP-EASTERN DIV  
77 A STREET  
NEEDHAM, MA 02194

GENERAL ELECTRIC COMPANY-TEMP  
ATTN WILLIAM ALFONTE

ATTN: DASTAC  
C/O DEFENSE NUCLEAR AGENCY  
WASHINGTON, DC 20305

GTE SYLVANIA, INC.  
ATTN PAUL H FREDRICKSON  
189 B STREET  
NEEDHAM HEIGHTS, MA 02194

GENERAL RESEARCH CORPORATION  
ATTN ROBERT D HILL  
P.O. BOX 3587  
SANTA BARBARA, CA 93105

GTE SYLVANIA, INC.  
ATTN H & V GROUP MARIO A NUNEFORA  
189 B STREET  
NEEDHAM HEIGHTS, MA 02194

COPY AVAILABLE TO DDC DOES NOT  
PERMIT FULLY LEGIBLE PRODUCTION

GTE SYLVANIA, INC.  
ATTN HERBERT A ULLMAN  
189 R STREET  
NEEDHAM HEIGHTS, MA 02194

GTE SYLVANIA, INC.  
ATTN CHARLES H RAHS OTTON  
189 R STREET  
NEEDHAM HEIGHTS, MA 02194

GULTON INDUSTRIES, INC.  
ATTN ENGINEERED MAGNETICS DIV  
ENGINEERED MAGNETICS DIVISION  
13041 CERRISE AVENUE  
HAWTHORNE, CA 90250

HARRIS CORPORATION  
ATTN T L CLARK MS 4040  
HARRIS SEMICONDUCTOR DIVISION  
P.O. BOX 883  
MELBOURNE, FL 32901

HARRIS CORPORATION  
ATTN CAROL F DAVIS MS 17-220  
HARRIS SEMICONDUCTOR DIVISION  
P.O. BOX 883  
MELBOURNE, FL 32901

HARRIS CORPORATION  
ATTN WAYNE E CHARE MS 16-111  
HARRIS SEMICONDUCTOR DIVISION  
P.O. BOX 883  
MELBOURNE, FL 32901

HAZELTINE CORPORATION  
ATTN TECH INFO CTR M LAITE  
PULASKI ROAD  
GREEN LAWN, NY 11740

HONEYWELL INCORPORATED  
ATTN RONALD R JOHNSON A1422

GOVERNMENT AND AERONAUTICAL  
PRODUCTS DIVISION  
2600 RIDGEWAY PARKWAY  
MINNEAPOLIS, MN 55413

HONEYWELL INCORPORATED  
ATTN R J HELL MS S2572  
GOVERNMENT AND AERONAUTICAL  
PRODUCTS DIVISION  
2600 RIDGEWAY PARKWAY  
MINNEAPOLIS, MN 55413

HONEYWELL INCORPORATED  
ATTN HARRISON H MOBLE MS 725-54  
AEROSPACE DIVISION  
13350 U.S. HIGHWAY 19  
ST. PETERSBURG, FL 33734

HONEYWELL INCORPORATED  
ATTN MS 725- STACEY H GRAFF  
AEROSPACE DIVISION  
13350 U.S. HIGHWAY 19  
ST. PETERSBURG, FL 33734

HONEYWELL INCORPORATED  
ATTN TECHNICAL LIBRARY  
RADIATION CENTER  
2 FORBES ROAD  
LEYINGTON, MA 02173

HUGHES AIRCRAFT COMPANY  
ATTN BILLY CAMPBELL MS A-E-110  
CENTINFLA AND TEALE  
CULVER CITY, CA 90230

HUGHES AIRCRAFT COMPANY  
ATTN DAN RINDER MS A-0147  
CENTINFLA AND TEALE  
CULVER CITY, CA 90230

COPY AVAILABLE TO DDC DOES NOT  
PERMIT FULLY LEGIBLE PRODUCTION

HUGHES AIRCRAFT COMPANY  
ATTN KENNETH R WALKER MS D157  
CENTINELA AND TEALE  
CULVER CITY, CA 90230

KAMAN SCIENCES CORPORATION  
ATTN ALBERT P BRIDGES  
P. O. BOX 7463  
COLORADO SPRINGS, CO 80933

HUGHES AIRCRAFT COMPANY  
ATTN EDWARD G SMITH MS A620  
SPACE SYSTEMS DIVISION  
P.O. BOX 92919  
LOS ANGELES, CA 90009

KAMAN SCIENCES CORPORATION  
ATTN WALTER F ARE  
P. O. BOX 7463  
COLORADO SPRINGS, CO 80933

HUGHES AIRCRAFT COMPANY  
ATTN WILLIAM W SCOTT MS A1080  
SPACE SYSTEMS DIVISION  
P.O. BOX 92919  
LOS ANGELES, CA 90009

LITTON SYSTEMS, INC.  
ATTN JOHN P RETZLER  
GUIDANCE & CONTROL SYSTEMS DIVISION  
5500 CANADA AVENUE  
WOODLAND HILLS, CA 91364

IRM CORPORATION  
ATTN FRANK FRANKELSKY  
ROUTE 170  
OREGO, NY 13827

LITTON SYSTEMS, INC.  
ATTN VAL J ASPHY MS 47  
GUIDANCE & CONTROL SYSTEMS DIVISION  
5500 CANADA AVENUE  
WOODLAND HILLS, CA 91364

IRM CORPORATION  
ATTN HARRY MATHERS (DEPT M41)  
ROUTE 170  
OREGO, NY 13827

LOCKHEED MISSILES & SPACE CO INC  
ATTN DEPT M200 G H MORRIS  
P.O. BOX 504  
SUNNYVALE, CA 94088

ION PHYSICS CORPORATION  
ATTN ROBERT D EVANS  
SOUTH BEDFORD STREET  
BURLINGTON, MA 01803

LOCKHEED MISSILES & SPACE CO INC  
ATTN GEORGE F HEATH D/R1-14  
P.O. BOX 504  
SUNNYVALE, CA 94088

IRT CORPORATION  
ATTN MDC  
P.O. BOX 81087  
SAN DIEGO, CA 92138

LOCKHEED MISSILES & SPACE CO INC  
ATTN EDWIN A SMITH DEPT 5-25  
P.O. BOX 504  
SUNNYVALE, CA 94088

COPY AVAILABLE TO DDC DOES NOT  
PERMIT FULLY LEGIBLE PRODUCTION

MARTIN MARIETTA AEROSPACE  
ATTN MONA C GRIFFITH LTR MP-30  
ORLANDO DIVISION  
P.O. BOX 5837  
ORLANDO FL 32805

MARTIN MARIETTA AEROSPACE  
ATTN WILLIAM M MRS MP-413  
ORLANDO DIVISION  
P.O. BOX 5837  
ORLANDO FL 32805

MARTIN MARIETTA AEROSPACE  
ATTN JACK H ASHFORD MP-537  
ORLANDO DIVISION  
P.O. BOX 5837  
ORLANDO FL 32805

MARTIN MARIETTA CORPORATION  
ATTN PAUL G PAGE MAIL 8203  
DENVER DIVISION  
P.O. BOX 179  
DENVER CO 80201

MARTIN MARIETTA CORPORATION  
ATTN RESEARCH LTR 6617 JAY R MCKEE  
DENVER DIVISION  
P.O. BOX 179  
DENVER CO 80201

MARTIN MARIETTA CORPORATION  
ATTN BEN T GRAHAM MS PD-454  
DENVER DIVISION  
P.O. BOX 179  
DENVER CO 80201

MARTIN MARIETTA CORPORATION  
ATTN J E GOODWIN MAIL 0452 (UNCL ONLY)  
DENVER DIVISION  
P.O. BOX 179  
DENVER CO 80201

LOCKHEED MISSILES & SPACE CO INC  
ATTN L ROSSI DEPT 81-64  
P.O. BOX 504  
SUNNYVALE CA 94088

LOCKHEED MISSILES & SPACE CO INC  
ATTN PHILIP J HART DEPT 81-14  
P.O. BOX 504  
SUNNYVALE CA 94088

LOCKHEED MISSILES & SPACE CO INC  
ATTN BENJAMIN T KIMURA DEPT 81-14  
P.O. BOX 504  
SUNNYVALE CA 94088

LOCKHEED MISSILES AND SPACE COMPANY  
ATTN TECH INFO CTR D/COLL  
3251 HANGER STREET  
PALO ALTO CA 94304

LTV AEROSPACE CORPORATION  
ATTN TECHNICAL DATA CENTER  
BOUGHT SYSTEMS DIVISION  
P.O. BOX 6267  
DALLAS TX 75222

LTV AEROSPACE CORPORATION  
ATTN TECHNICAL DATA CTR  
P.O. BOX 5907  
DALLAS TX 75222

M.I.T. LINCOLN LABORATORY  
ATTN LEONA LOUGHLIN LIBRARIAN A-062  
P.O. BOX 73  
LEWINGTON MA 02173

COPY AVAILABLE TO DGC DOES NOT  
PERMIT FULLY LEGIBLE PRODUCTION

MITRE CORPORATION, THE  
ATTN LIBRARY

P.O. BOX 208  
BEDFORD, MA 01730

MCDONNELL DOUGLAS CORPORATION  
ATTN TECHNICAL LIBRARY  
POST OFFICE BOX 516  
ST. LOUIS, MISSOURI 63166

NATIONAL ACADEMY OF SCIENCES  
ATTN R S SHANE NAT MATERIALS ADVSY  
ATTN: NATIONAL MATERIALS ADVISORY BOARD  
2101 CONSTITUTION AVENUE  
WASHINGTON, DC 20418

MCDONNELL DOUGLAS CORPORATION  
ATTN TO ENDER  
POST OFFICE BOX 516  
ST. LOUIS, MISSOURI 63166

NEW MEXICO UNIVERSITY OF  
ATTN W H GRANEMANN (UNCLASS ONLY)  
DEPT. OF CAMPUS SECURITY AND POLICE  
1821 ROSA N.E.  
ALBUQUERQUE, NM 87106

MCDONNELL DOUGLAS CORPORATION  
ATTN STANLEY SCHNEIDER  
5301 BOLSA A ENDE  
HUNTINGTON BEACH, CA 92647

NORTHROP CORPORATION  
ATTN ROYCE T AHLBORT  
ELECTRONIC DIVISION  
1 RESEARCH PARK  
PALOS VERDES PENINSULA, CA 90274

MCDONNELL DOUGLAS CORPORATION  
ATTN TECHNICAL LIBRARY, CI-291/36-80  
3855 LAKEWOOD BOULEVARD  
LONG BEACH, CA 90846

NORTHROP CORPORATION  
ATTN JOHN M REYNOLDS  
ELECTRONIC DIVISION  
1 RESEARCH PARK  
PALOS VERDES PENINSULA, CA 90274

MISSION RESEARCH CORPORATION  
ATTN WILLIAM C HART  
735 STATE STREET  
SANTA BARBARA, CA 93101

NORTHROP CORPORATION  
ATTN VINCENT R DEHARTINO  
ELECTRONIC DIVISION  
1 RESEARCH PARK  
PALOS VERDES PENINSULA, CA 90274

MISSION RESEARCH CORPORATION-SAN DIEGO  
ATTN V A J VAN LINT  
7650 CONVOY COURT  
SAN DIEGO, CA 92111

NORTHROP CORPORATION  
ATTN GEORGE H TOWNER  
ELECTRONIC DIVISION  
1 RESEARCH PARK  
PALOS VERDES PENINSULA, CA 90274

MITRE CORPORATION, THE  
ATTN M E FITZGERALD  
P.O. BOX 208  
BEDFORD, MA 01730

COPY AVAILABLE TO DDC DOES NOT  
PERMIT FULLY LEGIBLE PRODUCTION

NORTHROP CORPORATION  
ATTN ORLE L CURTIS JR  
NORTHROP RESEARCH AND TECHNOLOGY CTR  
3401 WEST BROADWAY  
HAWTHORNE, CA 90250

R & D ASSOCIATES  
ATTN S CLAY ROGERS  
P.O. BOX 9695  
MARINA DEL REY CA 90291

NORTHROP CORPORATION  
ATTN DAVID W POCOCK  
NORTHROP RESEARCH AND TECHNOLOGY CTR  
3401 WEST BROADWAY  
HAWTHORNE, CA 90250

RAYTHEON COMPANY  
ATTN GAJANAN H JOSHI RADAR SYS LAB  
HARTWELL ROAD  
REDFORD, MA 01730

NORTHROP CORPORATION  
ATTN JOSEPH D RUSSO  
ELECTRONIC DIVISION  
2301 WEST 120TH STREET  
HAWTHORNE, CA 90250

RAYTHEON COMPANY  
ATTN HAROLD L FLESCHER

528 BOSTON POST ROAD  
SUDBURY, MA 01776

PALISADES INST FOR RSCH SERVICES INC  
ATTN RECORDS SUPERVISOR  
201 VARICK STREET  
NEW YORK, NY 10014

RCA CORPORATION  
ATTN GEORGE J BRUCKER  
GOVERNMENT & COMMERCIAL SYSTEMS  
ASTRO ELECTRONICS DIVISION  
P.O. BOX 800, LUGIST CORNER  
PRINCETON, NJ 08540

PHYSICS INTERNATIONAL COMPANY  
ATTN DDC COJ FOR CHARLES H STALLING  
2700 MERCED STREET  
SAN LEANDRO, CA 94577

RCA CORPORATION  
ATTN K H ZAININGER  
DAVID SANDOFF RESEARCH CENTER  
W. WINDSOR TWP  
201 WASHINGTON ROAD, P.O. BOX 432  
PRINCETON, NJ 08540

PHYSICS INTERNATIONAL COMPANY  
ATTN DDC COJ FOR JOHN H MONTGOMERY  
2700 MERCED STREET  
SAN LEANDRO, CA 94577

RCA CORPORATION  
ATTN E VAN KEUREN 13-5-2  
CAMDEN COMPLEX  
FRONT, COPPER STREETS  
CAMDEN, NJ 08012

POWER PHYSICS CORPORATION  
ATTN MITCHELL BAKER  
542 INDUSTRIAL WAY WEST  
P.O. BOX 626  
EATONTOWN, NJ 07724

RENSSELAER POLYTECHNIC INSTITUTE  
ATTN RONALD J GUTMANN  
P.O. BOX 965  
TROY, NY 12181

COPY AVAILABLE TO DDC DOES NOT  
PERMIT FULLY LEGIBLE PRODUCTION

ROCKWELL INTERNATIONAL CORPORATION  
ATTN DENNIS SUTHERLAND  
ELECTRONICS OPERATIONS  
COLLINS RADIO GROUP  
5225 C AVENUE NE  
CEDAR RAPIDS, IA 52406

RESEARCH TRIANGLE INSTITUTE  
ATTN ENG DIR MAYRANT SIMONS JR  
P.O. BOX 12194  
RESEARCH TRIANGLE PARK, NC 27709

ROCKWELL INTERNATIONAL CORPORATION  
ATTN MILDRED A BLAIR  
ELECTRONICS OPERATIONS  
COLLINS RADIO GROUP  
5225 C AVENUE NE  
CEDAR RAPIDS, IA 52406

ROCKWELL INTERNATIONAL CORPORATION  
ATTN GEORGE C MESSENGER F-61  
3370 HIRALOMA AVENUE  
ANAHEIM, CA 92803

SANDERS ASSOCIATES, INC.  
ATTN MICHAEL AITEL NCA 1-3234  
25 CANAL STREET  
WASHINGTON, DC 20060

ROCKWELL INTERNATIONAL CORPORATION  
ATTN JAMES E HELL MA10  
3370 HIRALOMA AVENUE  
ANAHEIM, CA 92803

SCIENCE APPLICATIONS, INC.  
ATTN LARRY SCOTT  
P.O. BOX 2351  
LA JOLLA, CA 92038

ROCKWELL INTERNATIONAL CORPORATION  
ATTN K F HULL  
3370 HIRALOMA AVENUE  
ANAHEIM, CA 92803

SCIENCE APPLICATIONS, INC.  
ATTN J ROBERT BEYSTER  
P.O. BOX 2351  
LA JOLLA, CA 92038

ROCKWELL INTERNATIONAL CORPORATION  
ATTN DONALD J STEVENS FA70  
3370 HIRALOMA AVENUE  
ANAHEIM, CA 92803

SCIENCE APPLICATIONS, INC.  
ATTN NOEL R BYRN  
HUNTSVILLE DIVISION  
2109 W. CLINTON AVENUE  
SUITE 700  
HUNTSVILLE, AL 35805

ROCKWELL INTERNATIONAL CORPORATION  
ATTN T B VATER  
5701 WEST IMPERIAL HIGHWAY  
LOS ANGELES, CA 90009

SCIENCE APPLICATIONS, INC.  
ATTN CHARLES STEVENS  
2680 HANOVER STREET  
PALO ALTO, CA 94303

ROCKWELL INTERNATIONAL CORPORATION  
ATTN ALAN A LANGENFELD  
ELECTRONICS OPERATIONS  
COLLINS RADIO GROUP  
5225 C AVENUE NE  
CEDAR RAPIDS, IA 52406

COPY AVAILABLE TO DDC DOES NOT  
PERMIT FULLY LEGIBLE PRODUCTION

SIMULATION PHYSICS, INC.  
ATTN ROGER G LITTLE  
41 "H" STREET  
RURLINGTON, MA 01803

STANFORD RESEARCH INSTITUTE  
ATTN ROBERT A ARHISTEAD  
333 RAVENSWOOD AVENUE  
MENLO PARK, CA 94025

SINGER COMPANY (DATA SYSTEMS), THE  
ATTN TECH INFO CENTER  
150 TOTOLA ROAD  
WAYNE, NJ 07470

STANFORD RESEARCH INSTITUTE  
ATTN PHILIP J DOLAN  
333 RAVENSWOOD AVENUE  
MENLO PARK, CA 94025

SINGER COMPANY, THE  
ATTN IRVIN GOLDMAN ENG MANAGEMENT  
1150 MC BRIDE AVENUE  
LITTLE FALLS, NJ 07424

STANFORD RESEARCH INSTITUTE  
ATTN MACHERSON MORGAN  
306 WYNN DRIVE, N. W.  
MUNTSVILLE, AL 35805

SPERRY FLIGHT SYSTEMS DIVISION  
ATTN D ANDREW SCHUB  
SPERRY RAND CORPORATION  
P.O. BOX 21111  
PHOENIX, AZ 85036

SUNDSTRAND CORPORATION  
ATTN CURTIS B WHITE (NY CLASS)  
4751 HARRISON AVENUE  
ROCKFORD, IL 61101

SPERRY RAND CORPORATION  
ATTN JAMES A INDA MS 41T25  
UNIVAC DIVISION  
DEFENSE SYSTEMS DIVISION  
P.O. BOX 3575 MAIL STATION 1931  
ST. PAUL, MI 55101

SYSTRON-DUNGER CORPORATION  
ATTN HAROLD P MORRIS  
1000 SAN MIGUEL ROAD  
CONCORD, CA 94518

SPERRY RAND CORPORATION  
ATTN CHARLES L CRAIG E,  
SPERRY DIVISION  
SPERRY GYROSCOPE DIVISION  
SPERRY SYSTEMS MANAGEMENT DIVISION  
MARCUS AVENUE  
GREAT NECK, NY 11020

SYSTRON-DUNGER CORPORATION  
ATTN GORDON R DEAN  
1000 SAN MIGUEL ROAD  
CONCORD, CA 94518

SPERRY RAND CORPORATION  
ATTN PAUL MARAFFINO  
SPERRY DIVISION  
SPERRY GYROSCOPE DIVISION  
SPERRY SYSTEMS MANAGEMENT DIVISION  
MARCUS AVENUE  
GREAT NECK, NY 11020

TEXAS INSTRUMENTS, INC.  
ATTN DONALD J HARUS MS 72  
P.O. BOX 5474  
DALLAS, TX 75222

COPY AVAILABLE TO DDC DOES NOT  
PERMIT FULLY LEGIBLE PRODUCTION